

C O P C A M S

Cognitive & Perceptive Cameras

Artemis-JU GA n°332913

D5.2 Advanced Manufacturing Applications Specification

WP5 –Applications & Field Tests

Editors:

Valentin Koblar (KTOR), Bogdan Filipič (JSI),
Martin Pečar (JSI), Christian Fabre (CEA)



Date: 2016-01-05 at 16:08

Version: v2.1

Status: Final - Public

CEA ref. number: LETI/DACLE/15-0902

<http://copcams.eu>

COPCAMS Partners

CEA	Commissariat à l'énergie atomique et aux énergies alternatives
TCS	THALES Communications & Security SA
TRT-FR	THALES Research & Technology France (repr. THALES SA)
INRIA	Institut national de recherche en informatique et automatique
CTTC	Centre Tecnològic de Telecomunicacions de Catalunya
CCTL	Concatel
IQU	Iquadrat Informatica S.L.
TECN	Tecnia Research & Innovation
TED	Tedesys Global S.L.
UC	Universidad de Cantabria
GUT	Politechnika Gdańska
JSI	Institut "Jožef Stefan"
DTU	Danmarks Tekniske Universitet / IMM
TRT-UK	THALES Research & Technology (UK) Ltd
QMUL	Queen Mary University of London
ASEL	ASELSAN Electronics Industry
KTOR	Kolektor Group d.o.o.
SOG	Sogilis
SQST	Squadrone system

Table of Contents

1	Introduction	5
2	Demonstrator tasks	6
2.1	Quality control tasks (KTOR, JSI)	6
2.1.1	Dimensional measurements of the copper base in graphite commutator production ..	7
2.1.2	Quality inspection of copper-graphite soldering	9
2.1.3	Measurement of the commutator mounting holes roughness	10
2.2	Object positioning in a cooperative multi-camera system with RF sensing capabilities (GUT)	12
2.3	Augmented reality task (TED)	13
2.4	Robot tracking task (UC).....	15
3	Demonstrator architecture and methodology	16
3.1	Quality control tasks (KTOR, JSI)	16
3.1.1	Software methodology	20
3.2	Object positioning task (GUT)	22
3.3	Augmented reality task (TED)	27
3.4	Robot tracking task (UC).....	29
3.4.1	System implementation	29
3.4.2	UML/MARTE Model.....	30
4	Related lab experiments	33
4.1	Quality control tasks (KTOR, JSI)	33
4.1.1	Quality inspection of copper-graphite soldering	33
4.1.2	Measurement of the commutator mounting holes roughness	38
4.2	Object positioning task (GUT)	41
4.2.1	CV based positioning of Active RFID Tag	41
4.2.2	RFID switch measurements.....	54
4.2.3	RFID ESPAR antenna	55
4.2.4	RF based localization	58
4.3	Augmented reality task (TED)	60
4.4	Robot tracking task (UC).....	61
5	Validation	64
5.1	State of the art at project start.....	64
5.1.1	Quality control tasks (KTOR, JSI)	64
5.1.2	Object positioning task (GUT)	65
5.1.3	Augmented reality task (TED)	68
5.1.4	Robot tracking task (UC).....	68
5.2	Targets at project end	70
5.2.1	Quality control tasks (KTOR, JSI)	70
5.2.2	Object positioning task	71
5.2.3	Augmented reality task (TED)	73
6	Current state of the demonstrator	74
6.1.1	Quality control tasks (KTOR, JSI)	74
6.1.2	Object positioning task (GUT)	74
6.1.3	Augmented reality task (TED)	75
7	Conclusion.....	75
	References.....	76

1 Introduction

Vision systems are present in the manufacturing applications for at least two decades. First machine vision systems were, with respect to the current applications, quite simple, offering limited functionality. Gradually, with increasing computational power, machine vision systems became more complex. Today's machine vision systems in manufacturing environments mostly consist of fixed function, configurable cameras that stream video to PC-based (and in some cases small embedded) gateways.

The Cognitive and Perceptive Camera Systems (COPCAMS) project explores a new approach to the machine vision system in manufacturing applications. In contrast to the "camera-PC" approach, COPCAMS project will use many-core programmable accelerator platforms to capture and process images and other signals and extract the relevant information. Since the processing will be done locally on the embedded platform, only extracted information will be transmitted over the network. This will reduce the amount of the information sent over the network and enable implementing distributed machine vision applications.

The role of *D5.2 Advanced Manufacturing Applications Specification* document is to demonstrate the tools and methodologies developed during the COPCAMS project and to specify the demonstration activities (field tests and prototype demonstrations) in advanced manufacturing applications. Individual field tests described in this document will be evaluated based on the success criteria defined in the document *D1.4 – Summary of Use Cases and Field Test Definition*. Tools developed in WP2 and described in D2.4 will be used during the development, implementation and optimization of the demo applications. The algorithms described in WP3 (D3.6), will be implemented to demonstrate the tasks presented in this document. T5.2 has strong connection also with the WP4, where the middleware of the platforms used in advanced manufacturing demo is described. Initially the STHORM platform was intended to be used for all demonstrations in the Advanced Manufacturing Applications. However, due to the delay in the availability of this platform demonstrators decided to use also alternative platforms.

The document is further organized as follows. The demonstration task from the field of the quality control, object positioning, augmented reality and robot tracking are described in Section 2. Section 3 describes the proposed system architecture and methodology used in the design and evaluation of the field tests and demonstrations. The results of the preliminary experiments, performed in the laboratories, are presented in Section 4. In Section 5, the overview of the COPCAMS solutions in advanced manufacturing applications is presented, by comparing state of the art at the project start and the expected progress during the project. Section 6 summarizes the current state of the demonstrators and their tasks. Finally, Section 7 concludes this deliverable.

2 Demonstrator tasks

This section describes the field tests in *Advanced Manufacturing Applications*, which are defined in *D1.4 – Summary of Use Cases and Field Test Definition* document. The objective of *Advanced Manufacturing Applications* field tests is to show how the technologies developed during the COPCAMS project can improve the manufacturing process and implement solutions which are beyond the state of the art.

The demonstrator tasks in *Advanced Manufacturing Applications* are divided into four areas:

- Quality control tasks,
- Object positioning task,
- Augmented Reality (AR) task,
- Robot tracking task.

The demo in *Advanced Manufacturing Applications* will include four field tests and two prototype use cases. The field tests (quality control task and object positioning task) will be performed in a real-world manufacturing process at the KTOR production facilities. The AR task and robot tracking task will be demonstrated as an application prototype.

2.1 Quality control tasks (KTOR, JSI)

The aim of the quality control tasks is to develop and implement advanced machine-vision based quality control systems. Selected use cases will validate COPCAMS solution on the commutator production line at various stages of the production process and will partially substitute manual quality control. All three use cases are from the field of the product quality control and share same use-case diagram. The use-case diagram of the quality control tasks is shown in Figure 1.

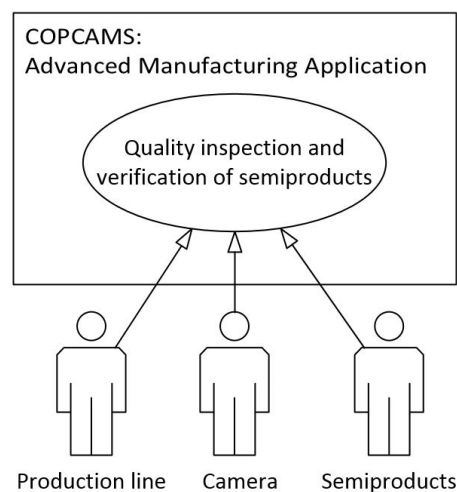


Figure 1: Quality control tasks use-case diagram

Each quality control task will include the following actors:

- Production line
- Camera / COPCAMS platform
- Semiproducts

2.1.1 Dimensional measurements of the copper base in graphite commutator production

Graphite commutator (Figure 2) is assembled from a copper base and a graphite body. In the initial production phase, the copper base is produced from a copper strip in the process of cold forming. The copper base has a relatively complex shape and many tolerances have to be checked before the subsequent phases of commutator production. The production cycle of the copper base is about 1 second per piece. The objective of the demo is to implement dimensional quality control of the copper base, based on predefined tolerances within the current production cycle.

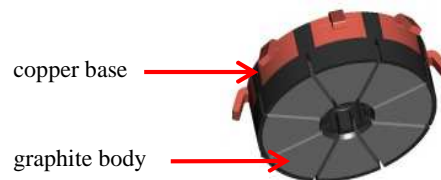


Figure 2: Graphite commutator

The copper base image captured with backlight illumination and marked dimensions, which have to be checked, is shown in Figure 3. Since the copper base contains eight symmetrically shaped anchors, every dimension has to be checked multiple times. For clearer representation, in Figure 3 each dimension is marked only once. The description of the dimensions with tolerances is listed in Table 1.

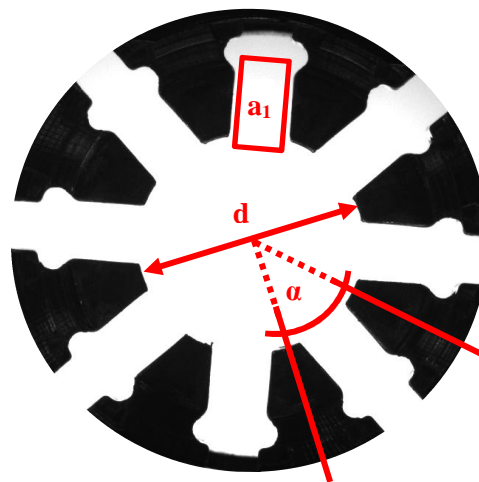


Figure 3: Captured image of the copper base with marked critical dimensions

Table 1: Critical dimensions with specified tolerances

Dimension (label in Figure 3)	Tolerances	Description
d_1	9.5 ± 0.25 mm max. difference between segment pairs < 0.3 mm	distance between two opposite anchors
α_1	$45^\circ \pm 1^\circ$	angle between two adjacent anchors
a_1	acceptable / unacceptable	area without the copper inclusions

The first dimension which has to be measured is the distance between the two opposite anchors. This dimension is crucial, since inadequate dimension results in improper alignment of the copper base with the graphite body. This can lead to a mechanical fault of the commutator. The copper base for the considered type of commutator consists of eight identical anchors. As shown in Figure 3 this dimension is measured between the two opposite anchors. Beside the absolute value of the dimension, also the maximal difference between the anchor pairs is important.

The next dimension, which has to be checked, is the angle between the adjacent anchors. Like the distance between the two opposite anchors, the angle between the anchors affects the alignment of the copper base with the graphite body, and consequently the mechanical strength of the produced commutator.

The last measurement that has to be verified is the presence of the copper inclusions in the area between the two adjacent anchors on the copper base. The copper base is produced in a process of cold forming. Since the copper base has a complex shape, unremoved copper may remain on the copper base. As a result, two adjacent anchors on the produced commutator can be short-circuited.

Performance of this use-case will be evaluated based on the following success criteria:

- accuracy of measurements/detections,
- software development and deployment cost,
- power consumption compared to currently used PC-based machine vision system.

2.1.2 Quality inspection of copper-graphite soldering

One of the phases of graphite commutator production is soldering of metalized graphite body (Figure 4), representing the brush track to the copper base. The process of soldering is one of the most critical processes in commutator production, since the reliability of the end user application directly depends on the strength of the copper-graphite joint. In the commutator production at KTOR, there is currently no automated quality control of the soldering process and all the commutators are inspected manually.



Figure 4: Graphite disc

To overcome the drawbacks of the manual inspection, we aim to design an automated quality control procedure for graphite commutator soldering process. Soldering process in commutator production consists of several phases. First, the right quantity of the soldering paste has to be applied to the specific area of the metalized graphite disc. Next, the graphite disc and the copper base are appropriately positioned and oriented, and then joined together. After both components have been joined, they are heated and a soldered joint is formed. Finally, the semiproduct is released to the next production phase on the commutator production line. The process of soldering takes about 5 seconds per piece.

During the soldering phase, four types of defects may occur:

1. metallization defect, i.e., there are visible defects on the metallization layer of the graphite body,
2. excess of solder, i.e., solder is split over the copper base,
3. deficit of solder, i.e., graphite body and the copper base are not properly soldered together,
4. disorientation, i.e., the copper part is not appropriately oriented with respect to the graphite part.

Each type of defect can occur only on a specific part of the commutator. Consequently, different types of defects can be identified on different segments of the commutator.

Defects, which occur during the soldering process, cannot be directly measured. Therefore, a domain expert has to manually classify a particular commutator into the appropriate quality class, i.e., define the type of defect.

Performance of this use-case will be evaluated based on the following success criteria:

- accuracy, confusion matrix of the deployed algorithm,
- software development and deployment cost,
- power consumption compared to currently used PC-based machine vision system.

2.1.3 Measurement of the commutator mounting holes roughness

Dimension and roughness of the mounting hole are two of the most critical characteristics of a commutator. When the commutator is mounted on an electrical motor shaft, a predefined force has to be achieved. This force depends on both characteristics – dimension and roughness of the mounting hole. In the demo, we will address the problem of measuring the roughness of the mounting hole (Figure 5) using machine vision. Usually, for roughness measurements, contact methods are used, but these methods tend to be very sensitive and are not suitable for on-line roughness measurement in production. On the market, there are also non-contact methods for roughness measurements available, such as scanning electron microscopy (SEM) and atomic force microscopy (AFM). These methods can provide very accurate measurements, but since they require preparation of the testing samples and are very sensitive to vibrations, they are not suitable for on-line roughness measurements. The objective of the demo is to develop and implement a machine vision based method for on-line, noncontact roughness measurement. Processing time of the commutator mounting hole is about 3 seconds per piece (including mechanical manipulation).

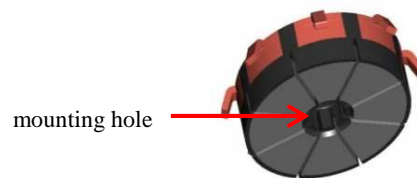


Figure 5: Graphite commutator with indicated mounting hole

A roughness value can be measured on a profile (line) or on a surface (area). There are different profile parameters available, which define how roughness is calculated from the measurements. The most common parameters are arithmetical mean deviation of the roughness profile (R_a) and maximum height of the roughness profile (R_z). The considered commutator mounting hole roughness is specified by the R_z parameter. The measured roughness value for this commutator should be less than 16 μm . The principle of calculating the R_z parameter is shown in Figure 6.

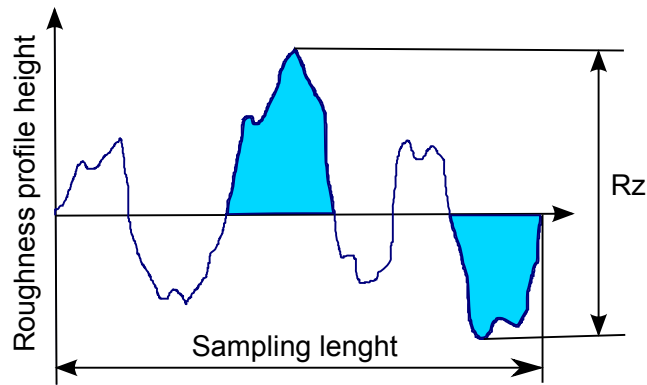


Figure 6: Calculation of the R_z profile parameter

The final treatment of the commutator mounting hole is done in the process of turning (Figure 7). In order to achieve the required quality of the mounting hole treatment, several parameters have to be set. These parameters are feed rate of the lathe tool, rotational speed of the semiproduct, etc. After these parameters for the specific type of commutator are determined, they are fixed and are not varied during the production process. The most significant factor that influences the hole roughness is the lathe tool wear. With the machine vision system that will measure the commutator hole roughness on-line, it will be also possible to monitor the wear of the lathe tool.

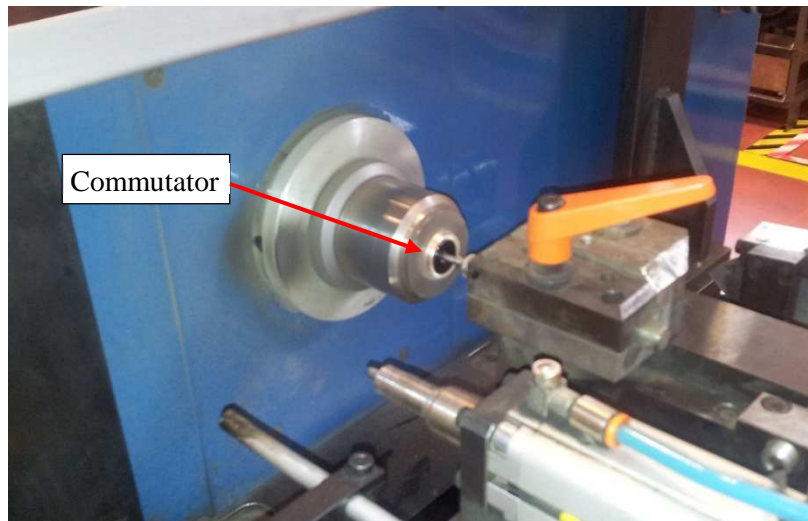


Figure 7: The final treatment of the commutator mounting hole

Performance of this use-case will be evaluated based on the following success criteria:

- accuracy, confusion matrix of the deployed algorithm,
- software development and deployment cost,
- power consumption compared to currently used PC-based machine vision system.

2.2 Object positioning in a cooperative multi-camera system with RF sensing capabilities (GUT)

Objective: In production facilities, information about assets position plays a key role in production efficiency. Real time or close-to real time position of assets, important in production process, may be used to limit the number of tools used, to decrease the time of tasks that have to be performed during production process or to improve the quality of the management process. In KTOR production facilities, RFID tags are to be attached to different assets (e.g. mobile tool cabinets, trolleys, plates, etc.), so they can easily be located in the production facility. The installed system of smart cameras with RF sensing capabilities will process the information gathered from RFID tags (active and/or passive) within the facility to determine the tags' position, and also to provide overviews and statistics of assets usage that can be used to help factory managers to optimize the production process. The objective of this use case is to test and assess the developed system of smart cameras having capability of RF signals sensing to support the production process. The use-case diagram of the quality control tasks is shown in Figure 8.

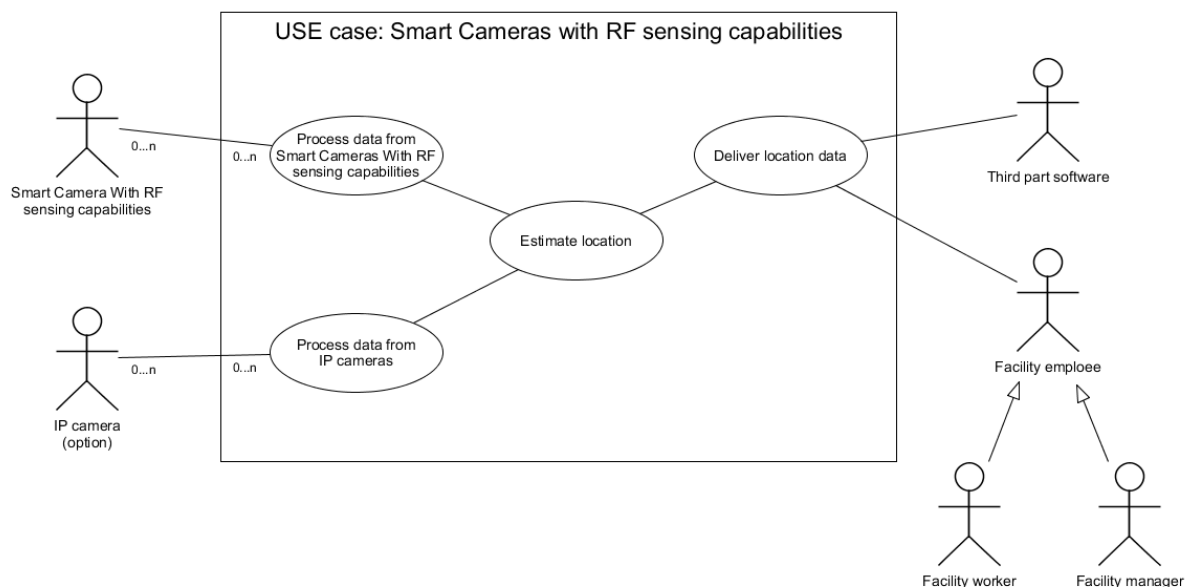


Figure 8: Object positioning system of Smart Cameras with RF sensing capabilities use-case diagram

Actors:

- Smart Cameras with RF sensing capabilities
- IP camera (optional, may not be present in the T5.2 demonstrator)
- Facility employee (e.g. facility manager, facility worker, etc.)

- Third party software (e.g. ERP, ERM, etc.)

Preconditions:

The system is correctly installed covering the area of interest (the system is using one or more cameras installed across the facility to detect assets, such as mobile tool cabinets, trolleys, plates , etc.

Post-conditions:

Success: Assets are correctly positioned/tracked providing the close to real-time information to facility manager/worker.

Failure: System is not able to provide assets localization and the possible reason is logged on sever.

2.3 Augmented reality task (TED)

This experiment explores the use of augmented reality (AR) as an aid in the execution of maintenance and repair works on machinery, computers hardware, electric equipment and other similar scenarios.

The main objectives of AR applied to maintenance and repair tasks is to improve productivity and to enable lower skilled technicians to perform specialized tasks. It is an area still at very early stage with only few pilot projects on the field and no real industrial deployment yet. Head-worn, motion-tracked displays augment the user's physical view of the system with information such as object labeling, guided steps, real time diagnostic data, and safety warnings. The virtualization of the user and maintenance environment allows off-site collaborators to monitor and assist with repairs. Additionally, the integration of real-world knowledge bases with detailed 3D models provides opportunities to use the system as a maintenance simulator/training tool.

All existing AR related trials are based on heavy computing equipment that limits the usability of the AR solutions. Indeed, many field applications only make sense if the equipment can be easily ported by the user (e.g. in army vehicles deployed in the field, remote oil rigs, etc.). Any efforts pushing this kind of extremely resource hungry applications towards more portable solutions (like, for instance, the COPCAMs platform) will facilitate future adoption by the industry.

The demonstrator under development will show the potential of this technology, especially in what involves the interaction between the image capture and analysis and the synthetic image generation, image blending and 3D display.

The application focuses on the optimization of the different building blocks, with special emphasis on the implementation of all image processing and analysis tasks on the GPU processor using standard

OpenCL. The value of this exercise lays in its direct portability to a range of embedded platforms that will facilitate the feasibility of future portable AR solutions by pushing the processing to the camera. This development will leverage the results of task T3.1 (Image processing algorithms).

The project will show the potential of AR as a human-machine interface and, moreover, the potential of AR to convey context dependent computer generated information to the user via the 3D immersive display.

The COPCAMS based system is composed of a virtual reality headset (Oculus Rift display) equipped with a stereo camera (Figure 9). The camera will stream the images to the headset allowing the user to navigate with the headset on using the 3D video feedback while those same images are sent to the COPCAMS platform where all tasks of image processing and object recognition are performed real time pushing parallel processing to the limit. Different object recognition algorithms will be applied allowing the system to provide an augmented reality experience by highlighting objects and providing related information.

The outcome of this processing is used to generate the information will appear in an overlay over the video feed providing help, guidance or important data of that object to the user in real time.



Figure 9: Virtual reality headset with front mounted stereo camera

2.4 Robot tracking task (UC)

The UC proposes a system and method to obtain the position of a robot/machine in an industrial environment applicable to any atmosphere (indoors or outdoors). This system comes under the advanced manufacturing applications' use case of COPCAMS project.

The system is based on the use of (Figure 10):

- light sources used as markers to calculate relative positions of the industrial machinery/robot,
- a stereo camera to display these markers in the image of the scene,
- an angle measuring device (as a gyroscope or electronic compass) to provide angles of rotation of the target object at each instant of time,
- and a digital signal processor, which uses the stored coordinates (from the memory) and output parameters obtained from the stereo camera and angle measuring device, to determine the target object position on the 3D environment.

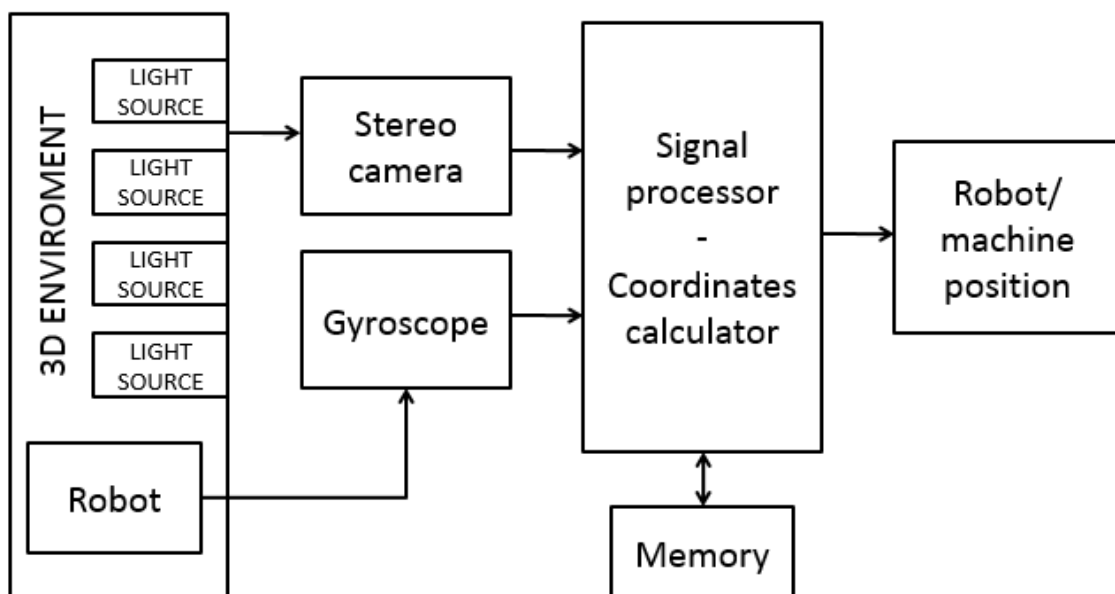


Figure 10: Schematic of the System Design

3 Demonstrator architecture and methodology

This section describes detailed architecture and methodology of the field tests, presented in the Section 2. Like the field tests, the architecture is divided into four major fields: architecture of the quality control tasks, architecture of the object positioning task, architecture of the AR tasks and architecture of the robot tracking task.

3.1 Quality control tasks (KTOR, JSI)

The demonstrations will be set up in the industrial environment in KTOR production facilities. During the demonstration design all safety and other technical recommendations will be considered. The production facilities, where the demonstration of the quality control task will be set up, is shown in Figure 11.



Figure 11: KTOR production facilities

The quality control tasks will demonstrate COPCAMS solutions in the KTOR production in the various stages of the commutator production process. Nevertheless, all quality control use cases will involve the following hardware elements:

1. COPCAMS platform (NVIDIA Jetson TK1)
2. IP camera with appropriate lens and illumination
3. Mechanical manipulator for the commutators
4. Automation elements for controlling quality control on the production line (PLC, sensors, etc.)

The selected platform for quality controls in KTOR is NVIDIA Jetson TK1 (Figure 12a) with 192 GPU cores. The platform will retrieve captured images from the camera, perform image processing and, based on the implemented classification model, classify commutators into the appropriate quality class.

NVIDIA Jetson TK1 platform supports OpenCV framework, where machine vision functions are already partially optimized for the implementation on the GPU. Currently, in KTOR all machine vision solutions are PC-based, with implemented machine vision algorithms running on the CPUs. The selected platform represents an alternative to the current solution and solution beyond the state of the art, since there are no available commercial GPU-based machine vision systems on the market.

In the quality control tasks the selection of the camera resolution, type of the lens and illumination are crucial. The camera resolution determines the minimal size of the defects that can be detected. The selected cameras have to be certified for the industrial environment usage and resistant to the electromagnetic interference (EMI) caused by the production lines. The selected IP Gigabit Ethernet (GigE) camera is shown in Figure 12b. For each use case, the lens and illumination will be selected based on the properties of the semiproduct and the type of the defects we want to detect. The choice of a suitable illumination is crucial to ensure constant and reliable analysis of the inspected parts. The selection of the lens and illumination will be done empirically.



Figure 12: Images of: a) NVIDIA Jetson TK1 platform, b) the selected IP GigE camera

In order to implement the quality control tasks to the selected production lines, adequate mechanical manipulators with the automation elements will be designed. These manipulators, incorporating Programmable Logic Controllers (PLCs), will communicate with the COPCAMS platform to ensure smooth operation of the production lines and provide the physical classification of the commutators. Manipulators with adequate automation elements will be designed in KTOR. Schematic representation of the connections between the system elements is shown in Figure 13.

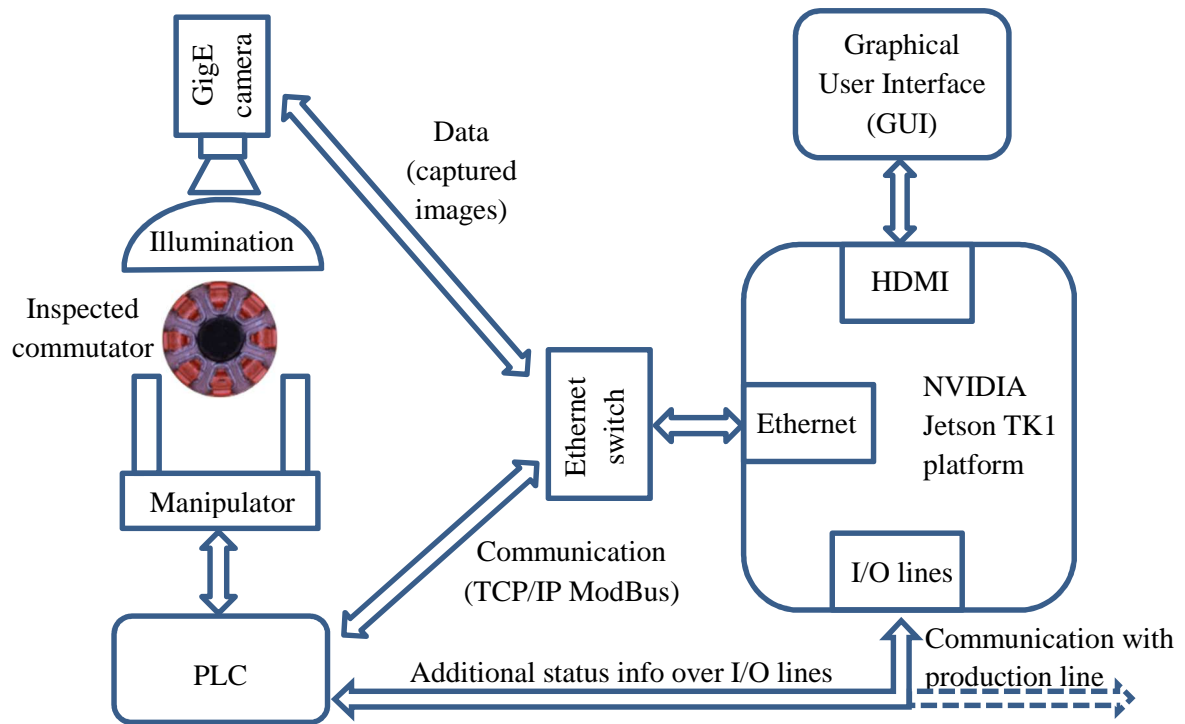


Figure 13: Schematic representation of connections between the system components

Three quality control tasks share identical architecture and methodology. Each use case scenario consists of the following actions:

- a) semiproduct is traveling along the conveyor belt,
- b) when the semiproduct reaches the predefined point on the production line (i.e. triggering point), it is transferred to the quality control system,
- c) images of the semiproduct are captured,
- d) machine vision algorithm extracts informative attributes,
- e) based on the attributes and pre-built classification model, semiproduct is classified into the appropriate quality class,
- f) semiproduct is either released back to the production line or eliminated from the production process.

The sequence diagram of the quality control task is shown in Figure 14.

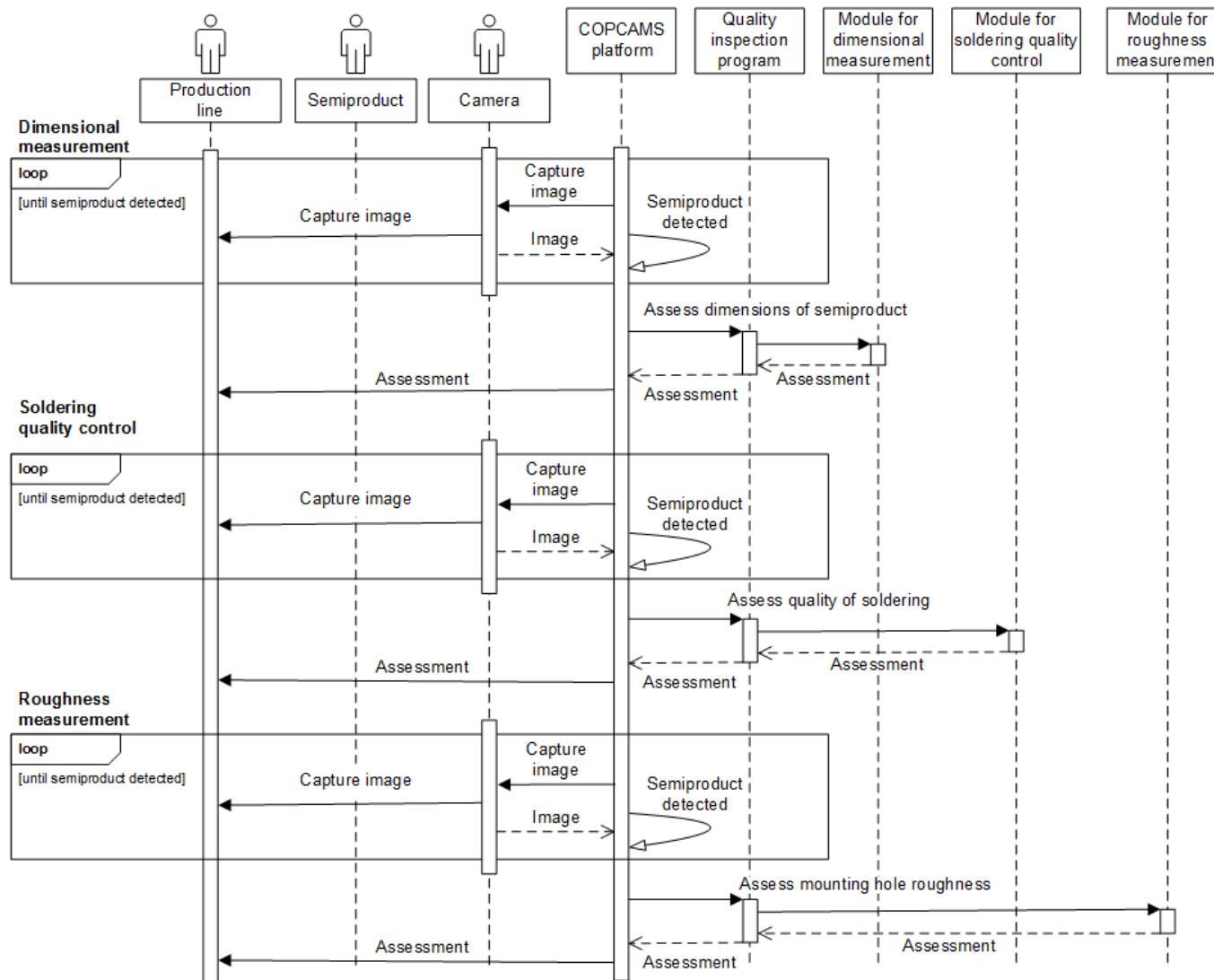


Figure 14: Quality control tasks sequence diagram

To allow undisturbed production of the commutators, all these actions have to be performed within the cycle time of the specific production process. The total cycle time is composed of the manipulation time, the commutator inspection and classification time. In order to ensure continuous operation of the production line, hardware and software have to be properly selected and configured.

The selected quality control tasks differ regarding the purpose of the demonstration and the methodology used for the task implementation. The dimensional task measurement serves as a validation of the selected platform and methodologies, and it is identified as a less complex task. The methodology in the soldering quality control task and roughness measurement task will be upgraded with ICT methodologies (machine learning and optimization methods) and will represent the software framework for developing new quality control applications based on the selected platform and developed methodology.

3.1.1 Software methodology

As described in Section 2.1.1 in the dimensional measurement task, three commutator characteristics have to be checked: distance between two opposite segments, angle between two adjacent segments and area without the copper inclusions (Figure 3). To measure the listed characteristic, dedicated machine vision algorithm will be developed and implemented on the NVIDIA Jetson TK1 platform. The concept of the software flow is shown in Figure 13.

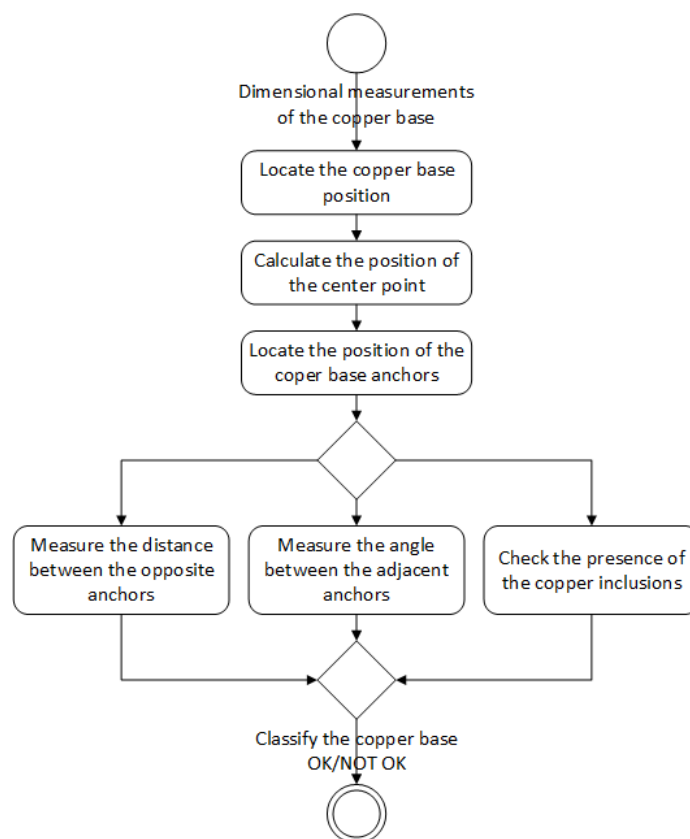


Figure 15: Software flowchart for the dimensional measurement task

The aim of the dimensional measurement task is to verify the described hardware infrastructure. Since the dimensional measurement task does not require the use of the advanced ICT methodologies, it is expected that will be the first use case implemented on the production line.

The soldering quality control task and roughness measurement task include advanced ICT techniques and share the same methodology in terms of constructing the classifier by combining computer vision, machine learning and evolutionary optimization techniques.

The methodology for automating these two quality control tasks is shown in Figure 16. It consists of three main stages: image processing, defect classification and tuning of the machine vision function parameters.

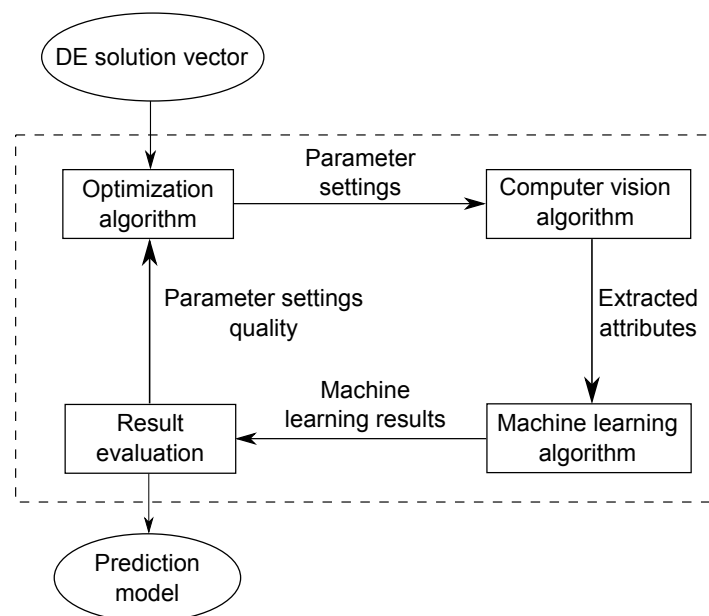


Figure 16: A schematic view of the proposed automated parameter tuning methodology

The image processing stage consists of several steps (e.g. capturing of images, region of interest (ROI) extraction, attribute/feature extraction) which will be adapted to the specific quality control task. In the defects classification stage, machine-learning algorithm builds classification models based on the attributes extracted with the machine vision algorithm. Their quality will be measured by the predefined fitness function (e.g. prediction accuracy). Depending of the problem type (classification or regression) the corresponding machine-learning algorithm will be selected. The last stage in designing the automated soldering control is tuning the machine vision function parameters. There are many optimization algorithms available for this task. As explained in detail in Section 4.1.1, for the preliminary tests we will use the Differential Evolution (DE) algorithm [5].

3.2 Object positioning task (GUT)

Object positioning in a cooperative multi-camera system with Radio Frequency (RF) sensing capabilities is a concept that expands the sensing capabilities of camera systems by adding means and algorithms to a smart camera system(s) that will allow them to “understand” and “interpret” RF waves present in the environment. One of the possible functionalities that are driven by industry needs and providing high added value (e.g. by optimizing production processes) is object positioning. To better understand object positioning in a cooperative multi-camera system with RF sensing capabilities and to ensure that the algorithms will address the business needs, the system concept will be presented using the environment where it will be finally installed for pilot tests (one of KTOR production facility). This is a large indoor environment with a large number of production machines. The pictures of the environment are presented below (Figure 17).

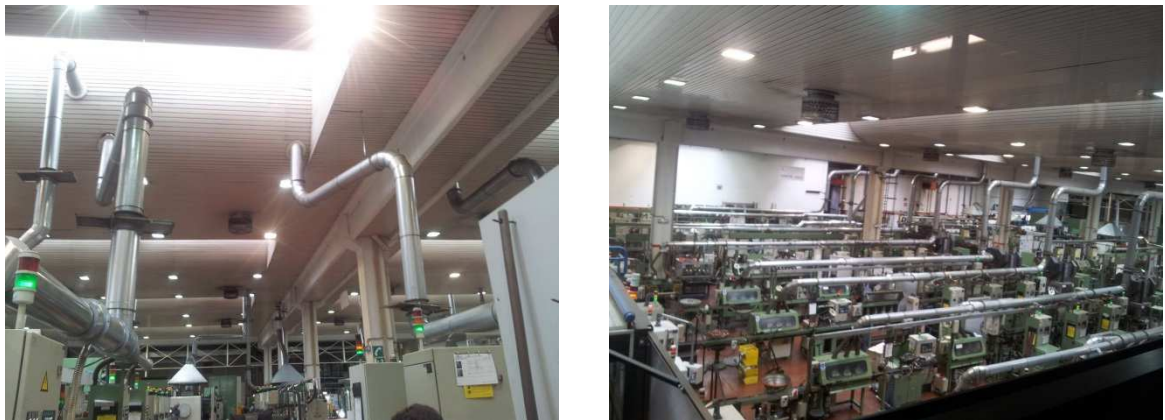


Figure 17: One of KTOR production facilities

According to information provided by KTOR representatives, there are three groups of objects that have been initially chosen as those to be localized (see Figure 18), namely:

- Plates
- Mobile tool cabinets
- Trolleys



Figure 18: Photos of exemplary plate, mobile tool cabinet and Trolley

The task of assets localization in one of KTOR industrial facilities brings many challenges and puts many requirements on the localization system. The background scene containing the production lines and workers can change dynamically and in an unpredictable way. The localized assets can be obscured not only unintentionally, but such situation is often the result of their typical functionality. Another attribute that characterizes every subgroup of localized assets is lack of distinctive features that are easy to observe by a vision system. Such environment can create many problems for typical Computer Vision algorithms and puts the necessity of use of other data sources that can provide useful support to the localization process. The use of measurements of radio signals parameters as an additional data source can help solve these problems, as radio signals are partially immune to no LOS (Line Of Sight) problem and their indoor behavior differs depending on the frequency. Moreover, the identification problem is very easy to resolve and an additionally radio based subsystem provides a very useful communication layer.

To fulfill all system requirements, the following system elements will be involved (Figure 19):

1. Integrated camera (the key element of the system).
2. Active RFID tags (2.4 GHz) with additional sensors/actuators
3. Passive RFID tags and readers (868 MHz)



Figure 19: Exemplary active RFID tags, passive RFID tags and cameras

The picture bellow (Figure 20) presents simplified connections between the localization system components based on a Smart Camera with RF sensing capabilities.

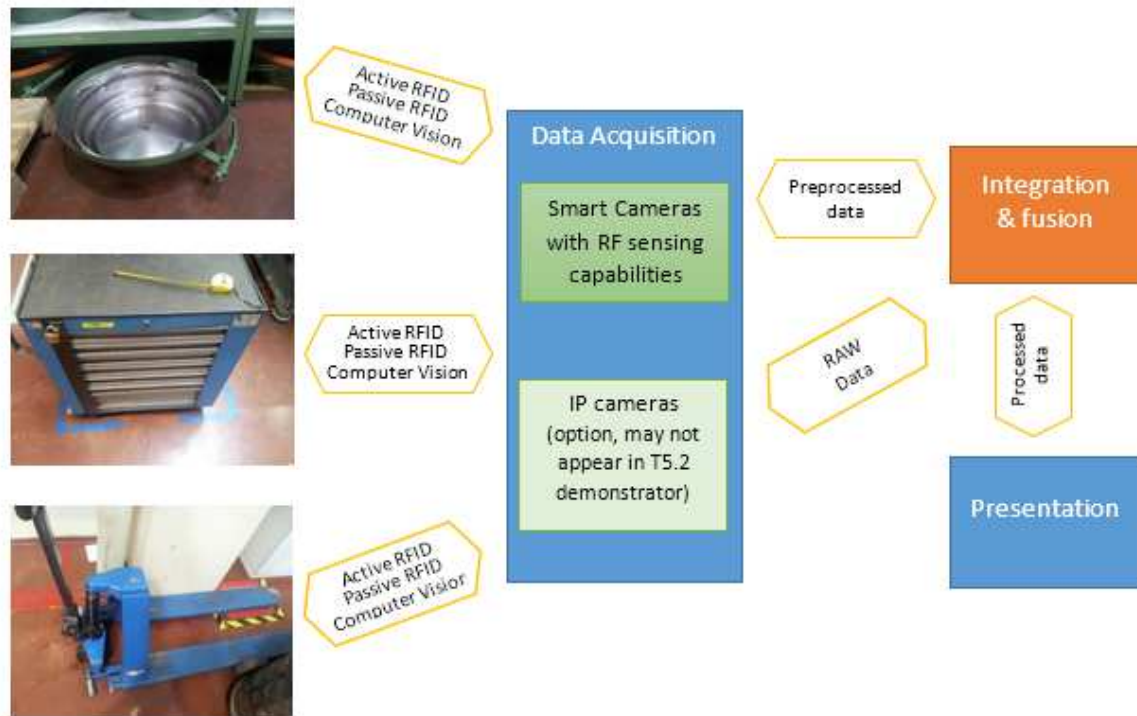


Figure 20: Simplified connections between the system components

Each of these technologies will provide localization data. Camera based Computer Vision may operate based on background subtraction algorithms (e.g. Gaussian Mixture Model) and in cooperation with active tags which will provide dynamic localization information using codes emitted by integrated light source (e.g. LED). Active tags will also allow for easy identification of object by the vision subsystem. Active RFID will provide information acquired from RF signal properties that includes RSS (Received Signal Strength). Measurement of these properties with cooperation with dedicated algorithms allows for calculation of object position in the investigated area. Passive RFID allows for localization based on proximity and together with dedicated antennas for determination of direction of signal arrival, the same as for active RFID.

To provide a clear view of the whole localization system, the list of components has been divided to three parts based on their functionality. Each part contains modules that provide necessary functionality and omits the issues like system calibration:

1. Smart Camera with RF sensing capacities
 - a. Integrated Camera
 - i. USB camera
 - ii. Active RF tag (2.4 GHz)
 - iii. Passive RFID reader (868 MHz) [option, may not be present in the final version of device]
 - iv. multicore System on Chip (KeyStone2 platform)
 - b. Active RFID tags
 - i. RF module (2.4 GHz)
 - ii. Steerable LED
 - iii. UHF passive RFID sensing unit [option, may not be present in the final version of device]
 - iv. Passive RFID reader (868 MHz)
 - v. Passive RFID tags (868 MHz)
2. Integration & data fusion infrastructure
 - a. Computation server (for numerical computations)
 - b. Switch
3. Additional infrastructure
 - a. Power sources
 - b. Data presentation
 - c. IP cameras [optional, may not be present in the demonstrator]

Each of the enumerated parts fulfills its role in whole system. Smart Camera with RF sensing capabilities is a device that merges advantages of both vision and RF measurements. The Integrated Camera is an integrated device that has both vision and RF sensing capabilities and integrated computational unit (KeyStone2 mSoC). The main advantage of this device is its ability to gather all necessary measurement data and provide processed localization data. The necessary algorithms can be implemented to work on the device. These properties have huge impact on the whole system in terms of its reduced complexity and scalability. Integrated Camera being a component of Smart Camera with RF sensing capabilities will also have the capability of working in the arrays or meshes of same kind of devices. The main sense of cooperation is the exchange of raw or preprocessed measurements and management of the whole system.

Active RFID tag is an integrated device able to communicate with Integrated Cameras and Computation server. Its main purpose is integration of nearly all kind of data sources in one device (some of them indirectly) which allows for system complexity reduction and, what is most important, easier possibility of merging all kinds of data. Another very important advantage of such integration is

greater ability of adjusting data sources behavior depending on changing environmental conditions and simpler managing of whole system. Depending of role in the system Active RFID tag can be integrated in Integrated Camera, play the role of Active RFID that is being localized or be a standalone reference device.

Passive RFID tags together with Passive RFID readers are intended to work in places where the active tag will not be used or simultaneously. Active RFID tag, due to its functionality, has to have dimension and structure capable of containing all of its modules and provide them with a power source. Due to this fact, in places where not all active tag functionalities will be necessary or where dimensionality of data source device is extremely important, standalone devices will be used.

The role of Active RFID tags not being localized and passive RFID readers not being part of Integrated Camera is to extend smart camera with RF sensing capabilities, so that it is more flexible and adjusted to practical implementations and able to provide/analyze data information from places where the Integrated camera will not be used. We can distinguish three reasons of no Integrated Camera readers usage. The first reason is connected with its physical dimensions – if there is no place or possibility for placing Integrated Camera, then standalone devices should be used. The second reason is connected to the area of interest – if the part of environment we are interested in is too difficult or makes impossible some kind of data measurement, the usage of full capability sensing device will not be economically effective. The third reason is insufficient amount of Integrated Camera devices. If RFID Reader is not used as a part of Integrated Camera, Active RFID Tag provides an interface that allows communication with Integrated Camera.

The part called “Integration & data fusion infrastructure” is responsible for communication, system functionality, data integration and computational power. As Smart Cameras are capable of working as standalone devices, other data sources need external processing and the last stage of data fusion and integration need to be processed on device.

The last part called “Additional infrastructure” is not strictly connected with the Smart cameras with RF sensing capabilities system. This part represents an external device with software responsible for presentation of localization data with the end user system governance interface and additional devices necessary for system work, but does not provide functionality. Additional IP cameras that can be integrated with Smart Cameras with RF sensing capacities system and extend its operational region without usage of Smart Cameras devices are enumerated in this section.

Figure 21 presents a simplified diagram of system parts and data flow between the components. Some of solutions (marked with dashed line) are at this moment considered as optional and may not be implemented in the final version of system or in the T5.2 demonstrator.

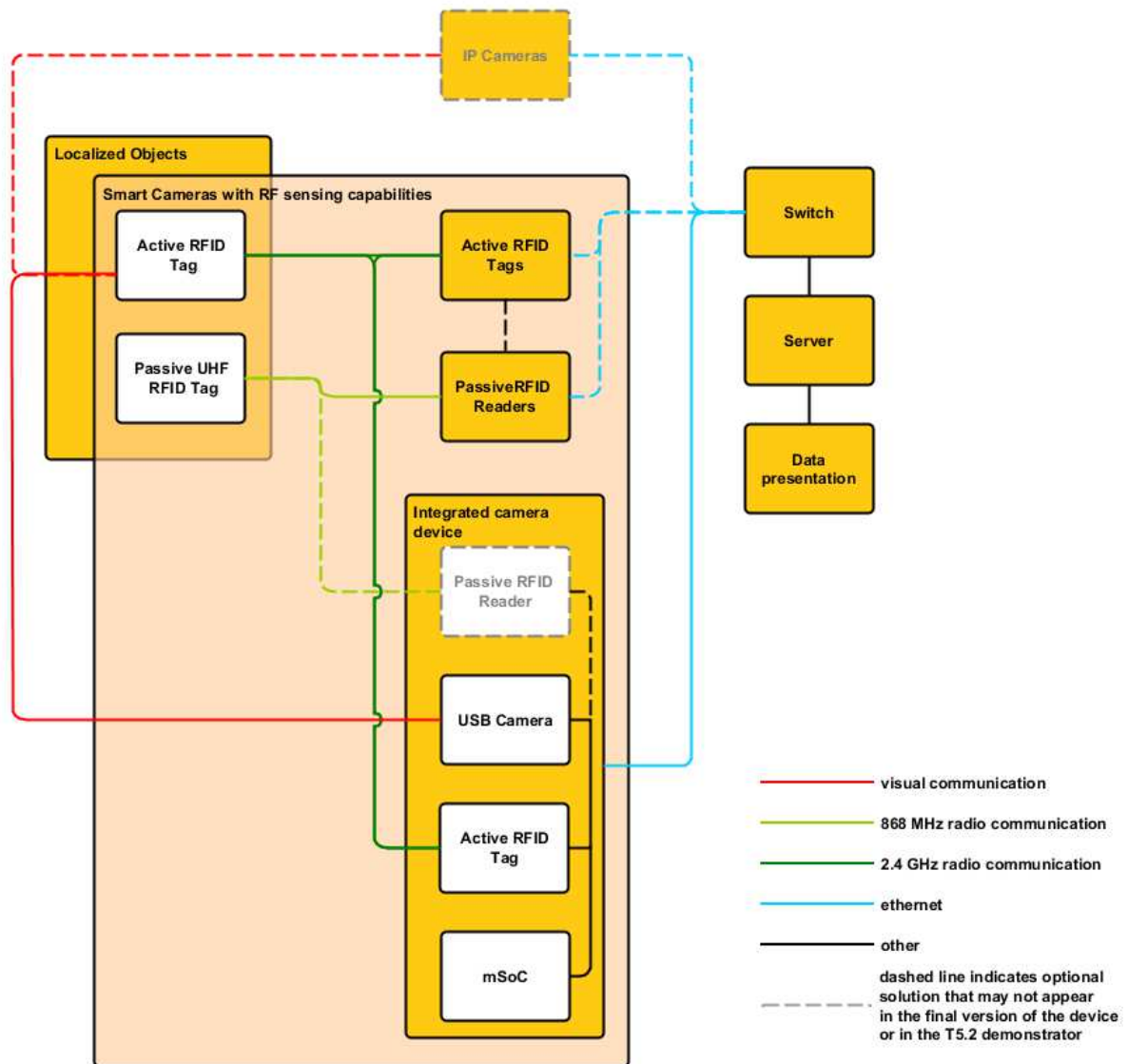


Figure 21: Simplified block scheme of expected system architecture and data flow

Processed localization, visual and radio data is collected in the computational server. Especially due to the fact that UHF RFID Readers and Active Tags are not part of Integrated Camera the server plays an important role in the whole system performance and capabilities. Computational server stores software responsible for system governance, some of data integration algorithms, localization algorithms (if not implemented in Integrated Cameras) and data storage.

3.3 Augmented reality task (TED)

The COPCAMS system will record and analyze the view of the system user through a stereo camera. In addition, for a proper posterior 3D visualization, images need to be undistorted and rectified. The COPCAMS platform will help also in this task.

The data processed by the COPCAMS platform will be sent to the NUC CPU for further processing, where a 3D image will be generated combining both the real data from the cameras and the augmented reality information generated in real time. The resulting images will then be projected to the headset where the user will perceive the illusion of seeing data integrated in his sight. The viewer will be developed using Unity3D because of the SDK for Oculus Rift headset usage. The architecture of the system is shown in Figure 22.

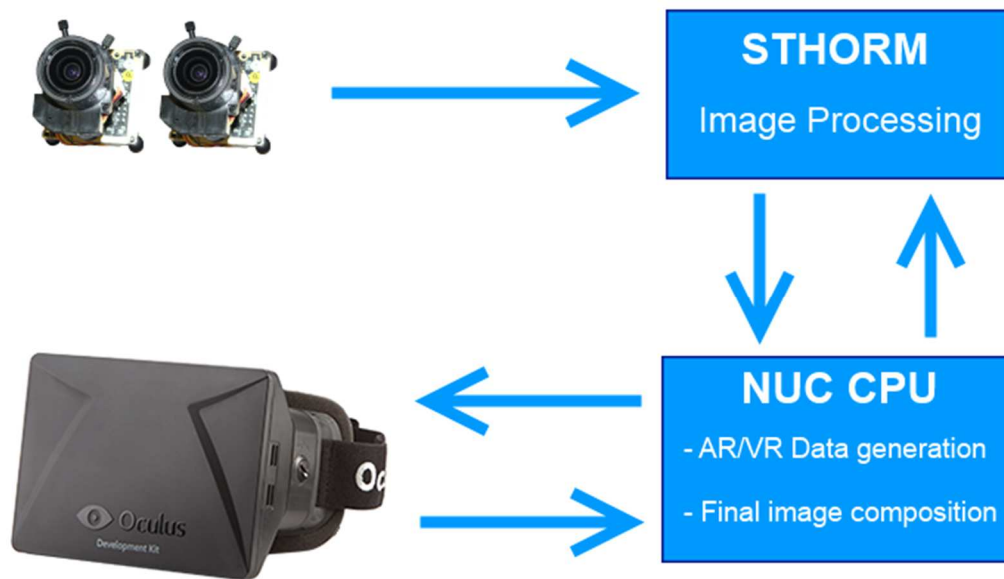


Figure 22: Demonstrator architecture

The COPCAMS platform will not only apply different preprocessing algorithms in order to produce undistorted and rectified images that will be provided to the NUC CPU for the 3D image generation, but will also run object recognition algorithms that will provide the NUC CPU with all the necessary information to generate the augmented reality scene.

The core object recognition algorithms developed will be based on key point model matching, although other alternative identification methods will be explored.

Image processing algorithms will be implemented using OpenCV and OpenCL to take full advantage of the COPCAMS platform.

This preprocessing will leverage the performance of the whole system, so the NUC can be used in visualization related CPU intensive operations like 3D scene generation.

3.4 Robot tracking task (UC)

3.4.1 System implementation

This section explains the system for obtaining, from the use of one or more luminous markers, the position and orientation of a user, in different possible environments, which may be indoor or outdoor, in a proposed controlled setting.

The method consists of different stages, where the input data from the cameras and gyroscope is processed to obtain the target object position. In the following lines, the data path is explained to understand how each phase treats data and obtains different output values.

- Stage 1: input data from the environment
 - Capture right and left images from the stereo camera
 - Obtain rotation angles from a gyroscope or an electronic compass

- Stage 2: detect movement and markers
 - Check the value of the gyroscope to know if the user has turned
 - Compare the current image frames and the previous image frame to notice movement from the user
 - Apply an algorithm to get the image coordinates of the reference markers and its radius (u, v, r) .

- Stage 3: identify movement type
 - Recognize the type of movement performed by the user, if it is frontal or horizontal, considering the markers radius.
 - Verify current markers coordinates by comparing them with the previous image region.

- Stage 4: this step is split in two sub-stages, depending on the type of movement detected.

Frontal movement:

- Obtain the distance (m) between the user and the marker by applying stereo triangulation.
- Obtain the distance (m) between the user and the marker by applying linear triangulation on the left image.
- Obtain the distance (m) between the user and the marker by applying linear triangulation on the right image.

Horizontal movement:

- Obtain the distance (m) of the horizontal displacement by applying a version of stereo triangulation (instead of taking two images of the same time sifted, it is going to use one image of the current time and another of the past time) on the left images.
 - Obtain the distance (m) of the horizontal displacement by applying a version of stereo triangulation on the right image.
 - Obtain the distance (m) of horizontal displacement by applying linear triangulation on the left image
 - Obtain the distance (m) of horizontal displacement by applying linear triangulation on the right image
- Stage 5: Get the user distance movement
 - Check and select the correct results of distances calculated on the stage 4, knowing the type of movement (frontal or horizontal), the type of displacement (if it is a frontal movement it can be an approaching or reprocessing from the marker and if it is a horizontal movement it can be right or left shift) and the number of detected markers on the image.
 - Stage 6: Obtain the target object position on the 3D environment
 - Get the final position by considering the data from the stage 5, the previous position and the user rotation.

3.4.2 UML/MARTE Model

In order to support all different stages of the flow, a powerful high-level methodology has been used. It is based on UML for development of HW/SW embedded systems; and the MARTE profile has been used to consider all the specific characteristics related to the embedded system design. This methodology can completely describe the system, enabling automatic generation of the input code. UML/MARTE model is based on graphical descriptions, which are called views. These views describe the system functionality, the target platform and the resource allocation. They are specified by the corresponding stereotypes:

1. Platform Independent Model (PIM) describes the functionality:
 - Data View,
 - Functional View,
 - Application View,
 - Concurrency View,
 - Memory Space View.

2. Platform Description Model (PDM) describes the platform where the functionality can be mapped:
 - HW Platform View,
 - SW Platform View.
3. Platform Specific Model (PSM) describes the mapping of the functional components in the platform:
 - Architecture View.

The work carried out on the first version of the model has been focused on the development of functional view, application view and architecture view and included a first definition of the system functions, their input and output signals, the relationship between those functions and the description of the selected platform.

- Functional View: in order to enable the communication between components, a set of services have been defined. These services are grouped into interfaces (Figure 23). These interfaces are specific for each inter-component communication channel (Figure 24).

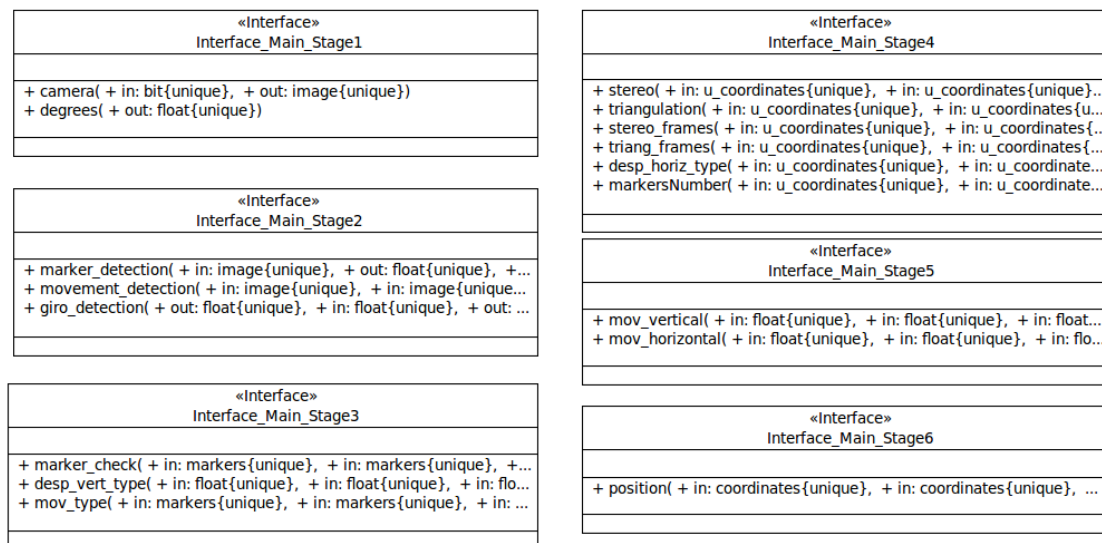


Figure 23: Interface diagram

- Application View: it shows the different components in the system and its relationship to others. A component offers a set of services (provided interface) and others components makes use of them (required interface).

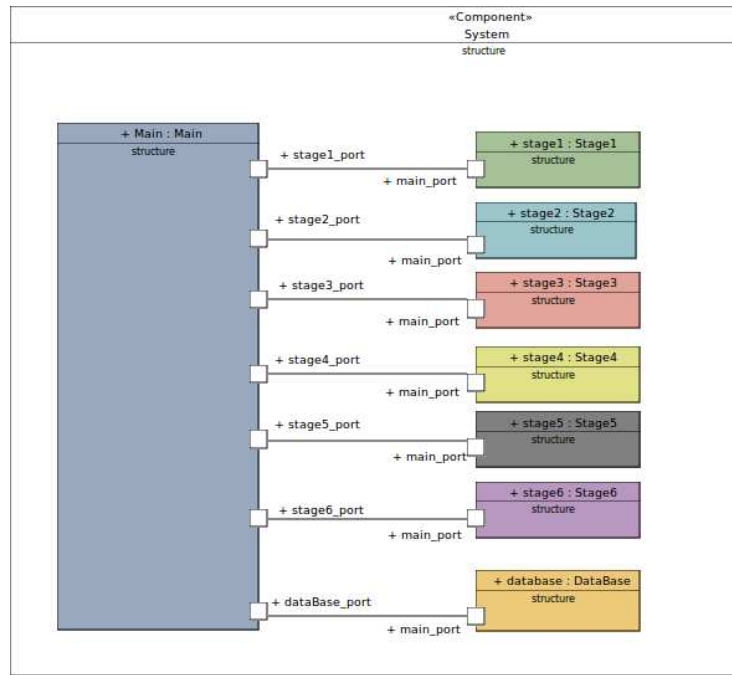


Figure 24: System application structure

- Architecture View: it is a platform specific model which defines the mapping of the functional components in the platform (Figure 25). It describes how the functionality was allocated on our development board, ODROID-XU3, which has 4 big cores (Cortex-A15) and 4 LITTLE cores (Cortex-A7).

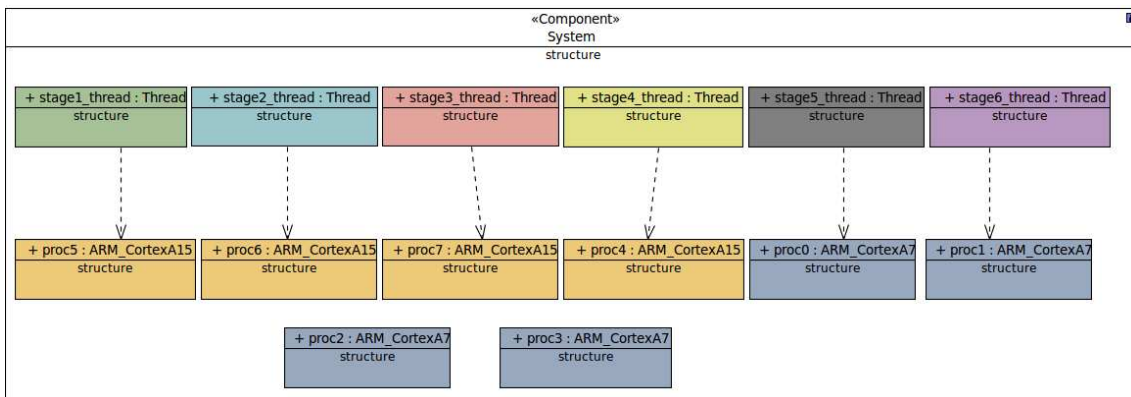


Figure 25: System mapping

It also includes the architecture of the development board (Figure 26). It describes the distribution of the elements, where processors Cortex-A7 (proc0-proc4) and processors Cortex-A15 (proc5-proc7) are connected to 2GB LPDDR3 RAM (RAM) through an AXI/AHB bus (main_bus), two bridges (bridge) and two AMBA buses (bus).

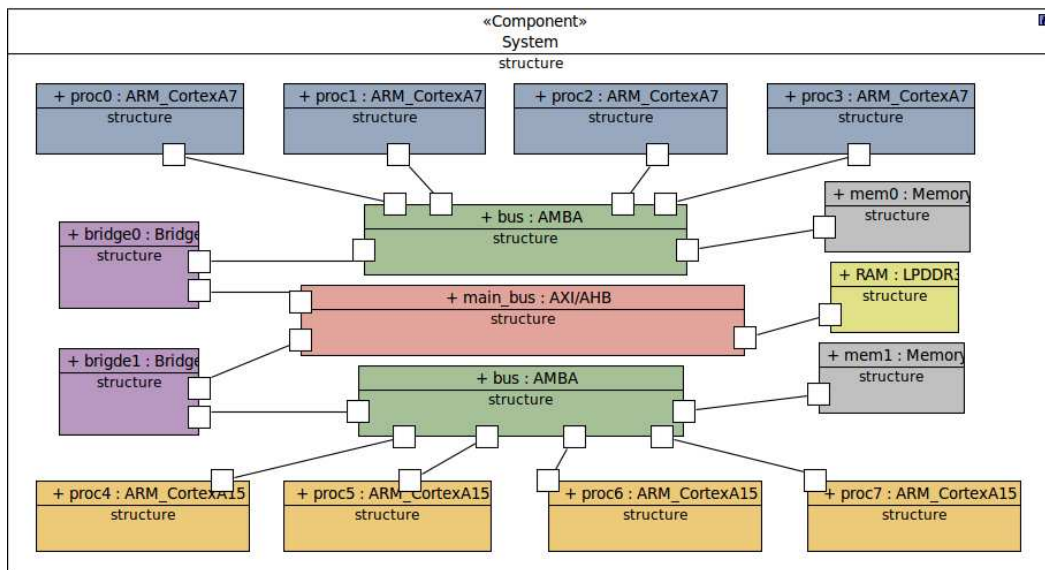


Figure 26: Platform architecture

4 Related lab experiments

4.1 Quality control tasks (KTOR, JSI)

4.1.1 Quality inspection of copper-graphite soldering

We are concerned with the estimation of the quality of copper-graphite joints in commutator manufacturing – a classification problem in which we wish to detect whether the joints are soldered well or have any of the four known defects:

- **Metallization defect:** presence of visible defects on the metallization layer,
- **Excess of solder:** presence of solder spots on the copper pad,
- **Deficit of solder:** lack of solder in the graphite-copper joint,
- **Disorientation:** disorientation between the copper body and the graphite disc.

Commutators consist of a number of segments, depending on the model (the considered commutator model from Figure 27 a) consists of eight segments). If a single segment has any of the listed defects, the whole commutator is labeled as defective and removed from the production process.

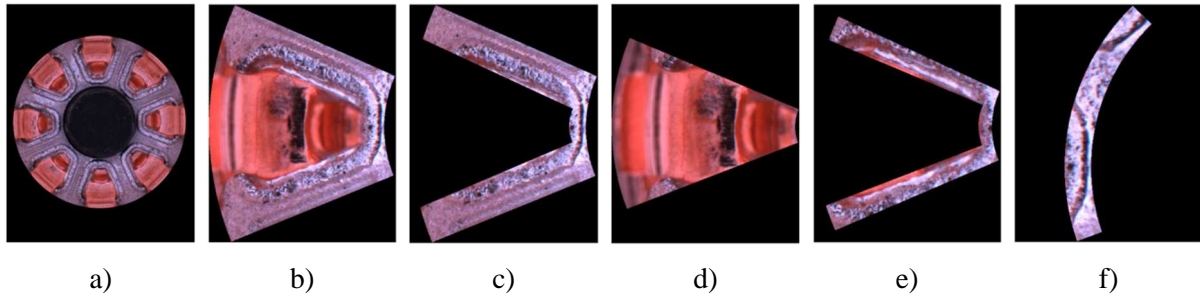


Figure 27: Images of: a) a graphite commutator, b) a commutator segment, c) a ROI for metallization defect, d) a ROI for excess of solder, e) a ROI for deficit of solder, and f) a ROI for disorientation

Different defects occur in different regions of the commutator segment. For example, the region where the excess of solder is usually detected is different from the region where disorientation can be observed. Therefore, images of commutator segments can be divided into four regions of interest (ROIs), one for each defect (see Figure 27).

Because five different outcomes are possible (rare cases where two or more defects appear on a single commutator segment are labeled with just one defect and are not differentiated further), we treat this as a classification problem with five classes. While KTOR is indeed interested in keeping statistics of the detected defects, their main concern is that no *false positives* are found. This means that cases when a defective commutator is labeled as without defects are to be avoided as much as possible. This is, of course, very hard to achieve.

4.1.1.1 Automated quality-control procedure

This quality-control procedure can be automated by means of an on-line classifier that can assess the quality of commutators as they are being manufactured. A classifier for this task can be constructed by combining computer vision, machine learning and evolutionary optimization techniques in the following procedure:

1. Define a set of image features.
2. Use an evolutionary algorithm to search for the values of image processing parameters that result in the highest fitness. Evaluate each solution using these steps:
 - a. Based on the chosen parameter values, use the image processing methods to convert each image of a commutator segment into a vector of feature values.
 - b. Construct a classifier (in our case a decision tree) where the vectors of feature values serve as learning instances. Estimate classifier performance and use this value as solution fitness.
3. Choose the best found classifier and the corresponding image processing parameters to detect defects in images of new commutator segments as they are being manufactured.

Let us now describe the steps of processing commutator segment images, building decision trees and optimizing classifier performance in more detail.

Processing commutator segment images

Processing of images is the most time consuming task of this procedure and is done in several steps. First, the image of the commutator segment needs to be properly aligned. Next, the four ROIs shown in Figure 27 need to be detected. This is done by applying four previously prepared binary masks to the image, one for each ROI. Each of the ROIs is further processed as follows. Depending on the ROI, the image in RGB format is converted into a gray-scale image by extracting a single color plane. Based on expert knowledge, red is used for all ROIs except the ROI for excess of solder, which uses the blue color plane.

The final three steps require certain parameters to be set. A 2D median filter of size 1×1 , 3×3 or 5×5 is applied to reduce noise. Next, a binary threshold that can take values from $\{1, 2, \dots, 256\}$ is used to eliminate irrelevant pixels. Finally, an additional particle filter is employed to remove all particles (connected pixels with similar properties) with a smaller number of pixels than a threshold value from $\{1, 2, \dots, 1000\}$. Note that because of the diversity of the defects, it is reasonable to assume that these three image processing parameters should be set independently for each ROI. This means that in total, 12 image processing parameters need to be set.

After these image processing steps, the chosen set of features is extracted from images of each ROI:

- number of particles,
- cumulative size of particles in pixels,
- maximal size of particles in pixels,
- minimal size of particles in pixels,
- gross/net ratio of the largest particle,
- gross/net ratio of the cumulative size of particles.

To summarize, computer vision methods are used to convert each commutator segment image into a vector of 24 feature values.

Building decision trees

Commutator segment images with known classes are used to construct a database of instances, upon which a machine learning classifier can be built. We chose decision trees since they are easy to understand and implement in the on-line quality-control procedure.

Note that the classifier predicts defects on commutator segments. For the final application, predictions for all segments of a commutator need to be aggregated in order to produce a prediction for the commutator as a whole.

Optimizing classifier performance

Classifier performance can be measured in several ways, ranging from classification accuracy, the F-measure to other, even custom functions that depend on the domain. Classification performance is estimated with 10-fold cross-validation, a popular technique for predicting classifier performance on unseen instances.

In order to find the values of image processing parameters that will result in a classifier with high accuracy, an evolutionary algorithm is employed to search in the 12-dimensional space of image processing parameter values.

4.1.1.2 Performed experiments

Here we report on lab experiments that were performed in order to test the suitability of the described automated quality-control procedure. While the studies had different experimental setups, they were all performed on the same commutator soldering domain with 363 instances and an uneven distribution of classes (see Table 2).

Table 2: The commutator soldering domain

Class	Number of instances	Frequency [%]
No defect	212	58.4
Metallization defect	35	9.6
Excess of solder	35	9.6
Deficit of solder	49	13.5
Disorientation	32	8.8
Total	363	100.0

The initial experiment [2] explored whether computer vision, machine learning and evolutionary optimization techniques could be employed to find small and accurate classifiers for this problem. The

DEMO (Differential Evolution for Multiobjective Optimization) algorithm [4] was applied to search for small and accurate trees by navigating through the space of decision tree parameter values, while the parameters of the computer vision methods were fixed to values chosen by an expert. Classifier accuracy was chosen to measure classifier performance. The study found this setup to be beneficial, but urged to focus future efforts on more sophisticated extraction of features from the images as this seemed to hinder the search for more accurate classifiers.

The second study [3] presented a different setup for the automated quality-control procedure to address the issues from the first study. Instead of optimizing decision tree parameter values, differential evolution (DE) [5] was used to search for the best setting of image processing parameters. The single classification problem with five classes was split into four binary classification sub-problems, where each sub-problem was dedicated to detecting one of the four defects and used data only from the corresponding ROI. In addition, instead of classification accuracy, the measure to be optimized was set to a function penalizing the portion of false negatives 100 times harder than the portion of false positives. The study found that the new combination of computer vision, machine learning and evolutionary optimization techniques was powerful and achieved some good results. While optimization with DE was always able to find better parameter settings for image processing methods than those defined by domain experts, some sub-problems proved to be harder than others. For example, detection of commutator segments with excess of solder achieved a satisfactory accuracy, while the detection of metallization defects did not.

The third study [1] investigated the correctness of the implicit assumption from [3] that only features of the sub-problem-specific ROI would influence the outcome of the classifier for that sub-problem. The study found that features from other ROIs can be important as well, suggesting that it might be better not to split the classification problem into sub-problems after all.

4.1.1.3 Lessons learned

Based on these lab experiments (and other experiments of smaller scale not reported here), we came to the following conclusions and suggestions for future work.

Suitable automated quality-control procedure

The experiments have proven that the designed automated quality-control procedure is indeed appropriate for this problem and we only need to fine-tune some of its elements to improve its performance.

Larger dataset needed

Most of the experiments have shown that the commutator soldering domain from Table 2 is not large enough for constructing more fine-grained classifiers with better performance. Therefore, we have already produced a larger dataset containing 533 commutators, corresponding to 4264 instances of the domain, which will be used to train the classifiers that will be finally implemented on the KTOR production line.

Need to improve detection accuracy for some defects

The difficulty of detecting a defect differs very much depending on the defect in question. For example, the excess of solder is much easier to detect than the deficit of solder for humans as well as for computer vision methods. While in the reported experiments classifiers often achieved satisfactory performance on some defects, results on other defects were not yet acceptable and more effort is required to improve them. Based on the findings of the previous studies, future work will be directed mostly towards the processing of commutator segment images, where different ROIs and new features should bring the sought improvement.

4.1.2 Measurement of the commutator mounting holes roughness

The aim of this task is to estimate the quality of the commutator mounting hole treatment. The validation of the treatment quality is done by measuring the roughness of the hole surface. For the specific commutator the allowed value of roughness is specified by the R_z parameter. This parameter may achieve maximum value of 16 μm . Commutators that have roughness of the mounting hole above this value are not acceptable and must be removed from the production process. Magnified mounting hole area is shown in Figure 28. The mounting hole surface can be presented as valleys and peaks along the measured surface.



Figure 28: Magnified commutator mounting hole area

In order to validate the feasibility of the mounting hole roughness measurement, several experiments were conducted. The problem of roughness measurement can be divided into the two type of tasks:

- a) Classification of the commutator into the appropriate binary class (commutators with adequate and commutators with inadequate mounting hole roughness),
- b) Prediction of the roughness value – regression.

According to the problem type (classification or regression problem), suitable measure for the accuracy must be selected. Since KTOR would like to eliminate all inadequate parts from the production process, the *false positives* should be minimized. In case of prediction of the roughness value, the error of predicted value should be minimized.

4.1.2.1 Automated quality-control procedure

Similarly as inspection of the copper-graphite soldering, this quality-control procedure can be automated. An on-line classifier can assess the quality of the commutator mounting hole roughness as they are being manufactured. By combining computer vision, machine learning and evolutionary optimization techniques we can automate the procedure of building the classifier.

Processing Commutator Mounting Holes Images

In the real-world application, the processing of captured images is the most time consuming task. It is composed of several sequential steps in which machine vision algorithms are applied. To gain optimal results, certain parameters of these algorithms must be set. First, the image of the mounting hole has to be cropped to the desired size of ROI (Figure 28). Next, the 2D median smoothing filter is applied to reduce the noise on the image. To achieve the optimal results the filter size must be set correctly (size $1 \times 1, \dots, 100 \times 100$). After the image is filtered, certain features are extracted from the grey scale image. These features forms part of a feature vector, which is later used as an input to the machine learning algorithm. Next, a binary threshold is used to remove some additional irrelevant pixels. Since the input image is 8-bit grayscale image, the binary threshold can take values from $\{1, 2, \dots, 256\}$. Finally, second set of features are extracted from the binary image and added to the feature vector. In total, 7 image processing parameters need to be set.

The result after these image processing step is a feature vector, containing 25 different features of each captured image. Some of these are:

- number of valleys on the image,
- number of peaks on the image,
- distance between the adjacent valley and peak on the image,
- 8-bit grayscale value of the lowest valley,
- 8-bit grayscale value of the highest peak,
- calculated Fast Fourier Transform (FFT) values on the line profile along the measured surface,
- etc.

Building a classifier

The result of the above procedure is a database containing feature vectors of processed images. As described in Section 4.1.2, this task can be divided into two subtasks: classification and regression task. Based on the built database, the machine learning algorithm induces a decision model – a decision tree in case of the classification task or a regression tree in case of the regression task.

Optimizing classifier performance

To optimize the classifier performance an evolutionary algorithm is applied. The algorithm searches the 25-dimensional space of image processing parameter values and tunes them until the best fitness function value is achieved. The model performance is estimated with 10-fold cross-validation. The procedure is the same for the classification and regression task.

4.1.2.2 Performed experiments

To test and validate the presented methodology some initial experiments were performed. The experiments were performed on the commutator soldering domain with 300 instances and distribution as shown in Table 3. To obtain the reference values of the mounting hole roughness, all commutators mounting holes were measured with a stylus profilometer. Each mounting hole roughness was measured three times, and then averaged.

Table 3: The commutator mounting hole roughness domain

Class	Number of instances	Frequency [%]
Roughness $R_z \leq 16 \mu\text{m}$	159	53.0
Roughness $R_z > 16 \mu\text{m}$	141	47.0
Total	300	100.0

The initial experiment explored the possibility of employing computer vision, machine learning and optimization techniques for autonomous building of the binary classification model. The DE algorithm [5] was used to vary and search for the optimal settings of the machine vision function parameters, while parameters of the machine learning algorithm were set to the default values. The classifier performance was measured by the classification accuracy. The study found that DE algorithm rather quickly iterates to the solution, where classification is 100% accurate. Furthermore, optimized classifier was able to 100% classify the instances based on just one attribute – FFT frequency on the line profile along the measured surface.

After the validation of the proposed methodology on the binary classification problem, the regression problem was tackled. The goal of the regression task was to calculate the measured value of

the roughness. For this purpose, the regression trees algorithm was employed. The classifier performance was measured by the root mean squared error (RMSE). The DE was used to search for the best settings of the image processing parameters. Several runs of the DE were performed and the best run achieved the RMSE value of 0.94. Although this result is quite incentive, there are possibilities for improving the regression model (e.g. through the extraction of additional attributes from the image and optimization of the machine learning algorithm parameters).

Based on the performed lab experiments the feasibility of the measuring of roughness based on machine vision procedure was confirmed. Furthermore, the proposed methodology, which includes machine learning and optimization techniques, has proven to be successful in finding better classification model compared to the manual setting of machine vision parameters. However, the problem of the regression model accuracy will be further analysed.

4.2 Object positioning task (GUT)

4.2.1 CV based positioning of Active RFID Tag

To proof the concept of active tag positioning, several experiments were prepared. The main aim was to check the effectiveness of proposed methodology (see deliverable D3.6) in terms of processing time and a proper identification. Second aim was to mimic the conditions of real industrial hall and use a high-resolution cameras as well, to acquire large, reliable database of video sequences for future research.

The prototype positioning subsystem consisted of (Figure 29):

- **Control unit** – personal computer with appropriate software to provide communication between all other parts of the system (cameras, wireless tags and so on), to visualize results and to maintain overall performance.
- **Camera device** (with lens) to provide video stream of a scene. Mounted on a metal stand and placed adequately to the position of visual tags.
- **Wireless router/gateway** to provide network gate (IPv6) for JennetIP protocol.
- **Active Tag prototype** – mobile JennetIP devices with LED top-mounted on it.

In final solution functionalities of all components will be provided by system of Smart Cameras with RF sensing capabilities that are described in Subsection 3.2.

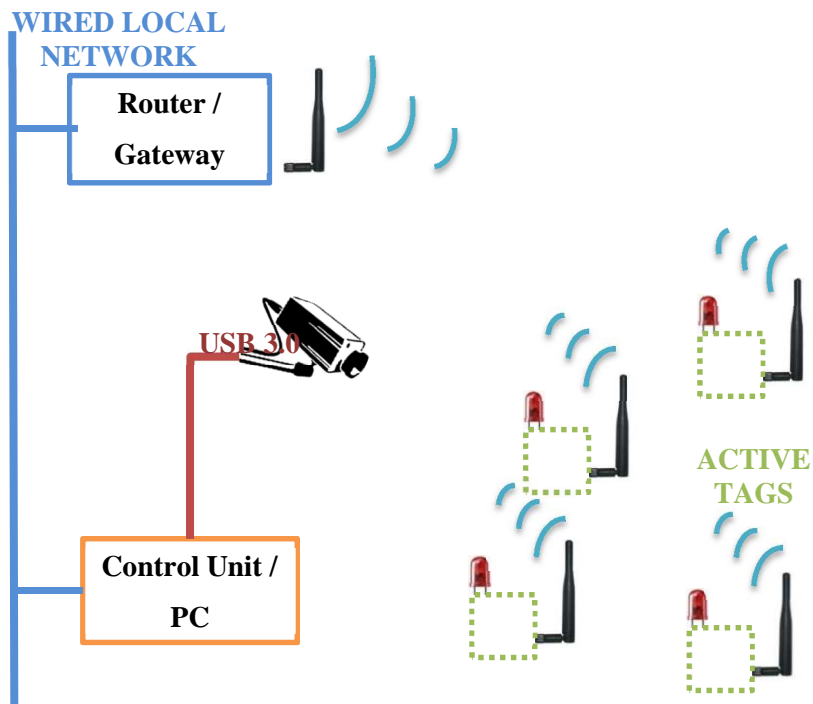
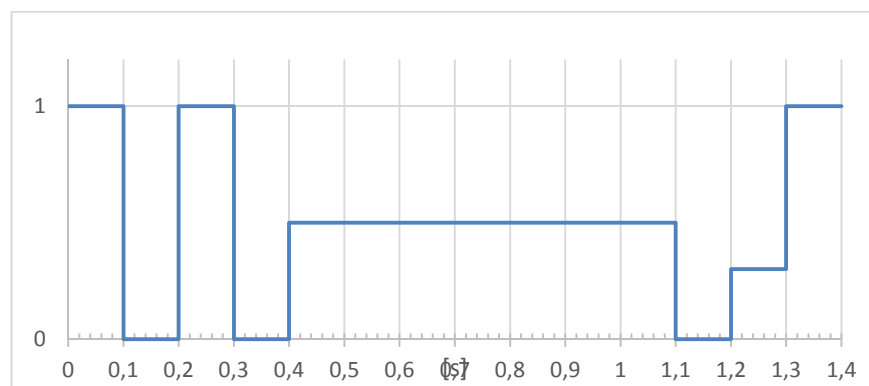


Figure 29: The scheme of developed positioning subsystem

We used simple amplitude-shift keying modulation to transmit signal from WLT to camera device. Symbol time was set to 100 ms, so the whole sequence took 1.4 s (Figure 30).



s0	S1	S2	S3	B0	B1	B2	B3	B4	B5	B6	S4	P	s5
1	0	1	0	X	X	X	X	X	X	X	0	X	1

Figure 30: Exemplary sequence transmitted as identification of Active Tag

S0, S1, S2, S3, S4, S5 – Constant synchronization bits.

B0, B1, B2, B3, B4, B5, B6 – Sequence data bits carrying a unique WLT identification.

P – Parity bit.

Proposed algorithm [21] was applied to acquired camera image. In Figure 31 the scene image and masks produced by algorithm stages are presented. In the last image all Tags are positioned (in image) and identified.

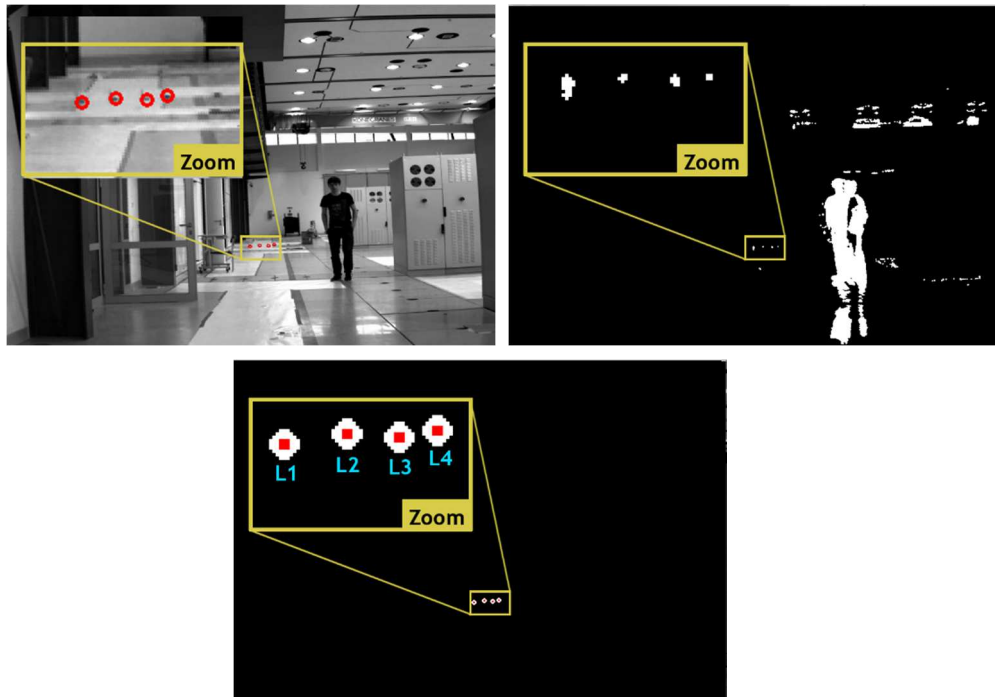


Figure 31: Exemplary steps of tag detection algorithm

4.2.1.1 *In-image tag positioning*

The first task was to examine the effectiveness of positioning tags on the camera image. Experiments were performed in “Linte²” laboratory located in the Faculty of Electrical and Control Engineering at the Gdansk University of Technology, that can be treated as fine reproduction of a common industrial hall (Figure 32). As the camera device Point Grey FLEA USB3.0 cameras were used.



Figure 32: The industrial hall used for test purposes

The aim of experiment was to prove efficiency of proposed algorithm in terms of processing time and accuracy. A few Active RFID Tags were placed in the camera field of view and localization command was triggered. Measurement procedure consists of the following stages:

1. Retrieving the list of currently available (connected) Active RFID Tags.
2. Sending unique blinking sequence to each of available Active RFID Tags.
3. Triggering localization procedure requested by user.
4. Start video stream acquisition from the camera.
5. Broadcast “start sequence” command to all available devices.
6. After calculated time, stop video acquisition.
7. Searching for known sequences in video buffer.
8. Matching sequences with corresponding devices.

The three simple performance indicators can be distinguished:

- **Overall measurement time** – duration of the whole measurement procedure: from pushing “start” button, to get tags positions (steps 3 – 8).
- **Video analysis processing time** – duration of computer vision algorithms (step 7).
- **Positioning efficiency** – ratio of correctly found and identified Active Tags in camera frame to all connected and visible devices.

Scenario 1



Figure 33: The result of WLT detection in scenario 1

In the first scenario all Active RFID Tags were placed on the floor 3 m away from the camera device in a room adjacent to the main hall (Figure 33). Light conditions were very good – illuminance at about 400 lx, smooth shades and not polished floor. Tags were lying about 5 – 10 cm from each other. The results are shown in Table 4.

Table 4: Scenario 1 results

Overall measurement time	2724 ms
Video analysis processing time	378 ms
Positioning efficiency	100 %
Video parameters	1280x1024 48 FPS

Scenario 2



Figure 34: The result of Tags detection in scenario 2

The second scenario was conducted in industrial hall where Active RFID Tags were placed at some different distances from camera (Figure 34). The furthest devices were placed 15 m from camera. Illuminance at about 300 lx was observed. The first problem was revealed – with a high FPS coefficients light flickering (that came from PWM-modulated LED lamps) was observed, but it has not spoiled the results. The results are listed in Table 5.

Table 5: Scenario 2 results

Overall measurement time	3106 ms
Video analysis processing time	403 ms
Positioning efficiency	100 %
Video parameters	1280x1024 50 FPS

Scenario 3

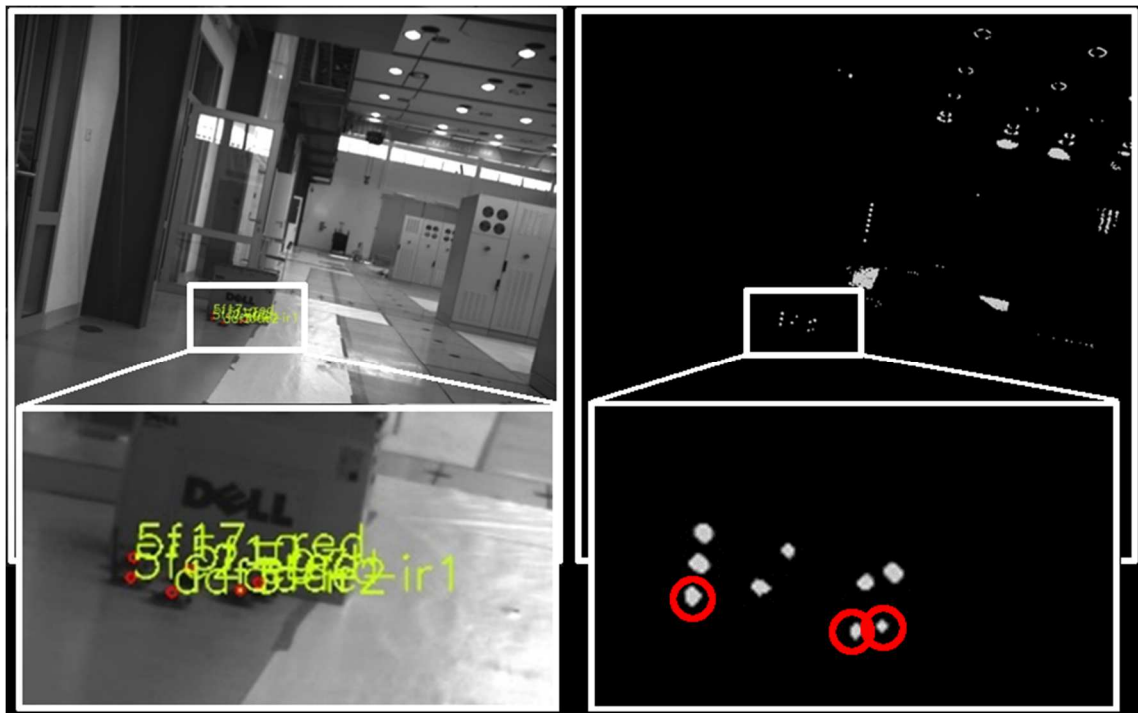


Figure 35: The result of Tags detection in scenario 3. Red circles are bad LED detection due to reflection phenomena

In this experiment Tags were placed at about 7 m from camera and very close to each other (3 – 7 cm). The floor was polished, thus reflection problem appeared, which is illustrated in Figure 35. The result of this scenario are shown in Table 6.

Table 6: Scenario 3 results

Overall measurement time	4543 ms
Video analysis processing time	1067 ms
Positioning efficiency	100 %
Video parameters	2048x2048 24 FPS

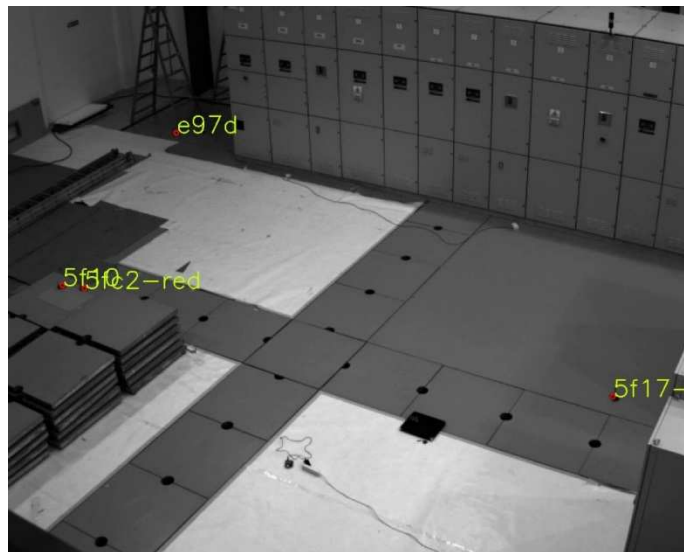
Scenario 4

Figure 36: The result of Tags detection in scenario 4

In this scenario the close to real industrial case was recreated in the test lab, so the camera was placed as high as possible with wide view on the scene. Active RFID Tags were placed randomly – in long and short distance from camera and each other (Figure 36). Tag “e97d” was situated about 25 m away from camera. The results are listed in Table 7.

Table 7: Scenario 4 results

Overall measurement time	2966 ms
Video analysis processing time	315 ms
Positioning efficiency	100 %
Video parameters	1280x1024 48 FPS

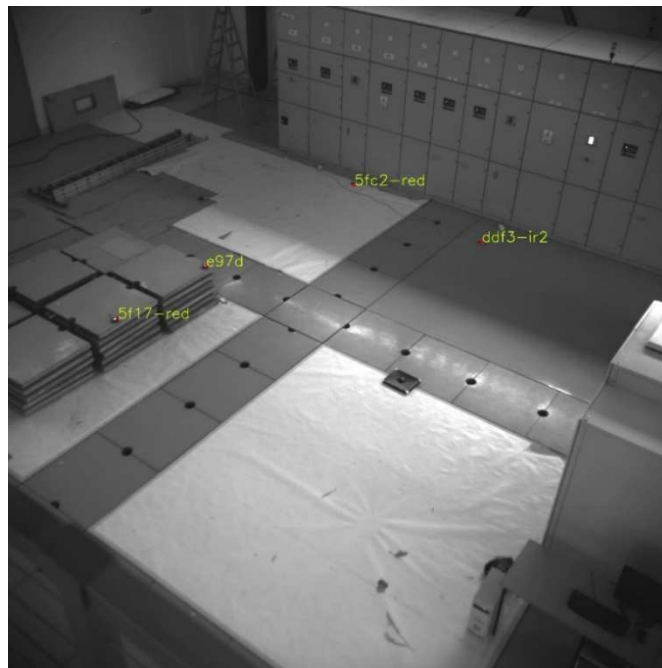
Scenario 5

Figure 37: The result of Tags detection in scenario 5

Table 8: Scenario 5 results

Overall measurement time	4052 ms
Video analysis processing time	816 ms
Positioning efficiency	100 %
Video parameters	2048x2048 26 FPS

Scenario 6

Figure 38: The result of Tags detection in scenario 6

In this experiment we placed Active RFID Tags in long distance from camera (about 20 m) and close to each other (about 5 cm). The results are listed in Table 9.

Table 9: Scenario 6 results

Overall measurement time	3015 ms
Video analysis processing time	488 ms
Positioning efficiency	100 %
Video parameters	1280x1024 45 FPS

4.2.1.2 Tags localization in a real-world coordinate system

In order to examine the solution in terms on effectiveness and reliability, the experimental setup was developed. Algorithms were implemented with use of C++ programming language and OpenCV image processing library to provide appropriate data-types, structures and basic algorithms (for detailed description of algorithms see deliverable D3.6). Large industry hall in the Faculty of Electrical and Control Engineering at Gdansk University of Technology was used as the experimental environment. The hall floorplan is shown in Figure 39. The reason for using such a location was recreating the real factory conditions. During the experiment, some encountered problems occurred:

- High overall brightness, which decreases contrast between tags' LED light and the scene lighting.
- Industrial hall lighting based on PWM-modulated LED lamps, which was generating some flickering in frames' brightness at high FPS sequences.
- Additional in-frame motion, which came from normal factory's daytime activities.
- High-reflective floor and some metallic equipment, which could mislead detection algorithm.

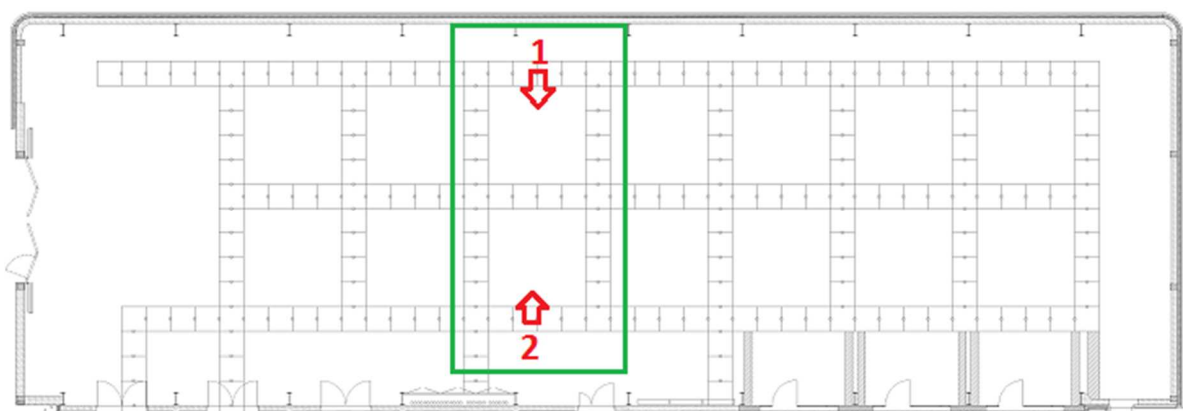


Figure 39: The map of the whole factory hall with the area of experiment (green box) and camera positions (red)

In the area of experiment, 14 Active RFID Tags were placed and localized with usage of implemented algorithm. Two types of cameras were used:

1. Point Grey GrassHopper3 USB3.0 1024x1024 with Fujinon lens,
2. Point Grey Flea3 USB3.0 1280x1024 with Fujinon lens.

The location of each camera is marked by green dot in Figure 40.

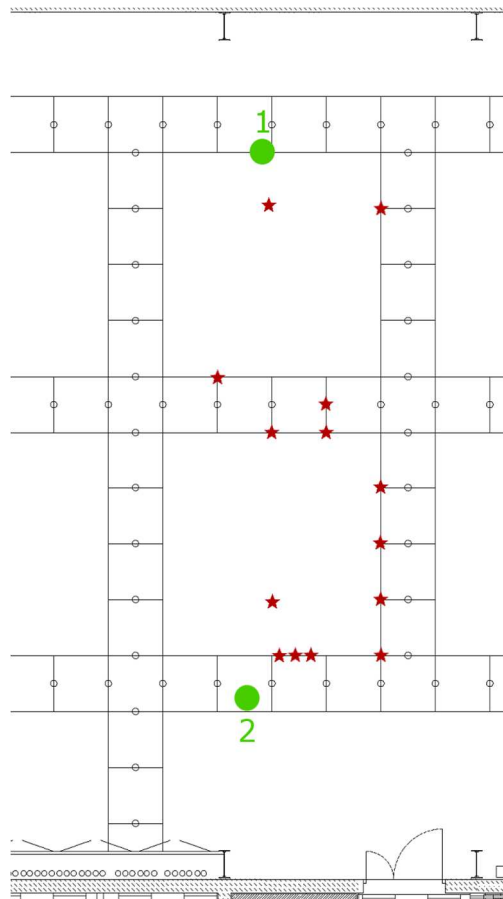


Figure 40: Active RFID Tags reference positions (red) and cameras (green)

In Figure 41, a view from Camera 1 is shown (without distortion correction). All tags were localized and identified. In Figure 42, one can see the results of transformation from image to map coordinate system. Calculated positions of tags are marked by red dots.

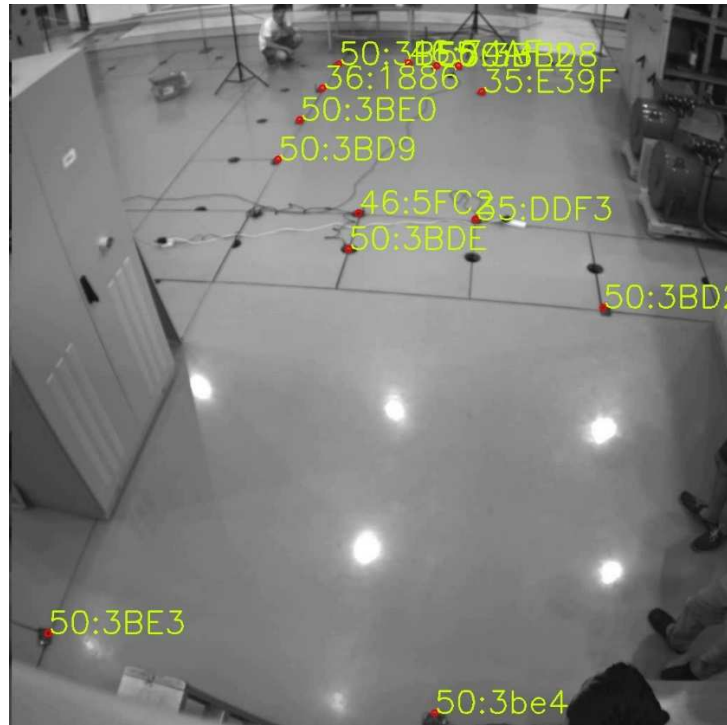


Figure 41: Camera 1: the result of computer vision algorithm(view without distortion correction)

Active RFID Tags are depicted by red dots and their IDs

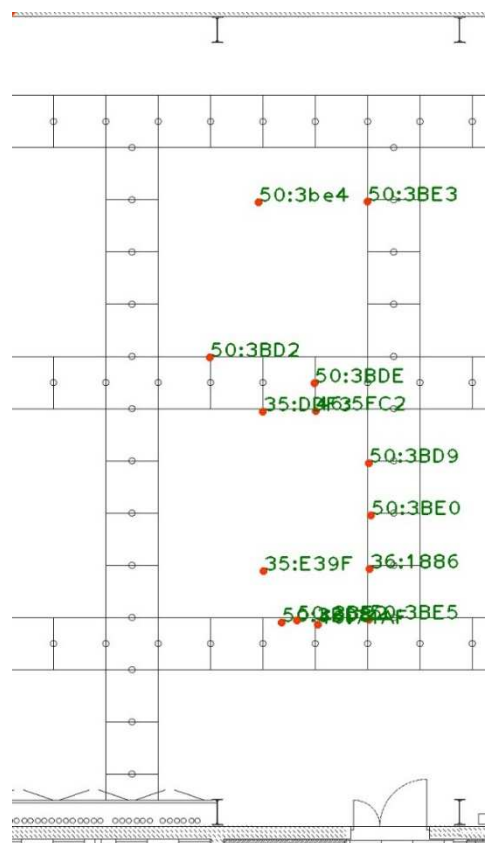


Figure 42: Camera 1: real-world positions of Active RFID Tags computed by distortion compensation and perspective transform algorithm

In Figure 43, a view from Camera 2 (without distortion correction) is presented. All tags were localized and identified. In Figure 44, results of transformation from image to map coordinate system are shown. Calculated positions of tags are marked by red dots.

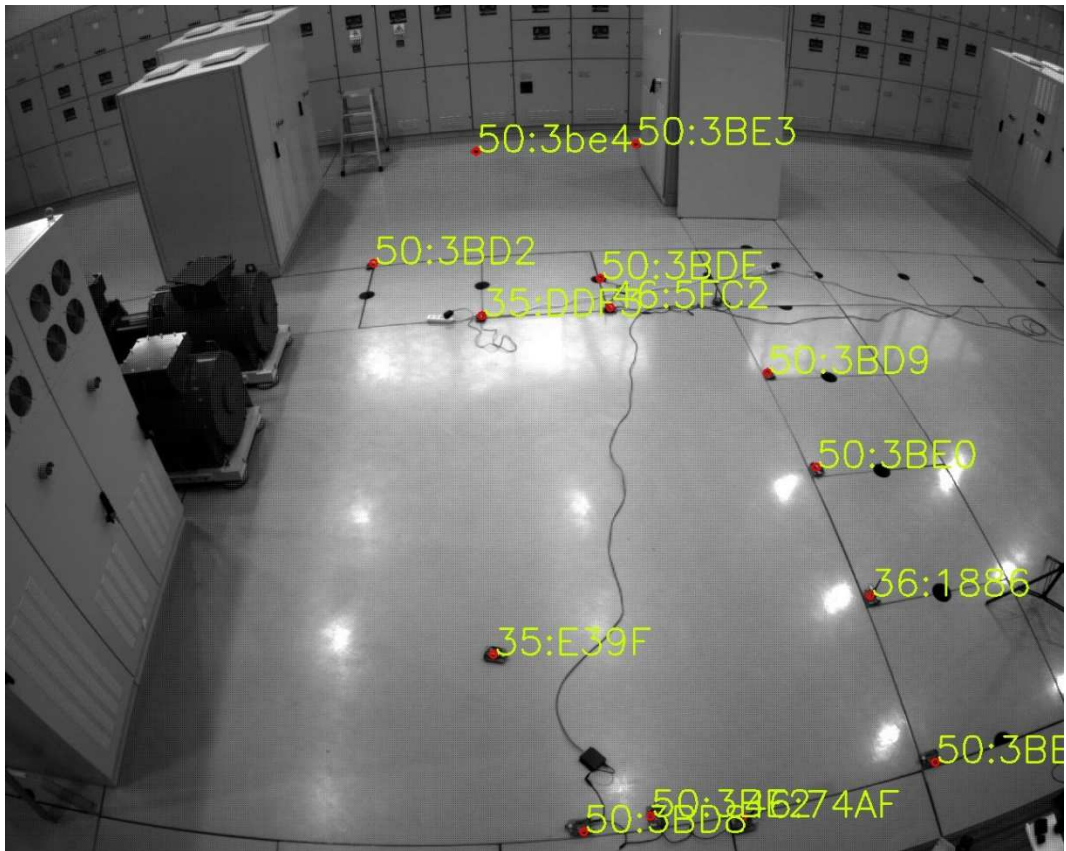


Figure 43: Camera 2: the result of computer vision algorithm (view without distortion correction). Active RFID Tags are depicted by red dots and their IDs

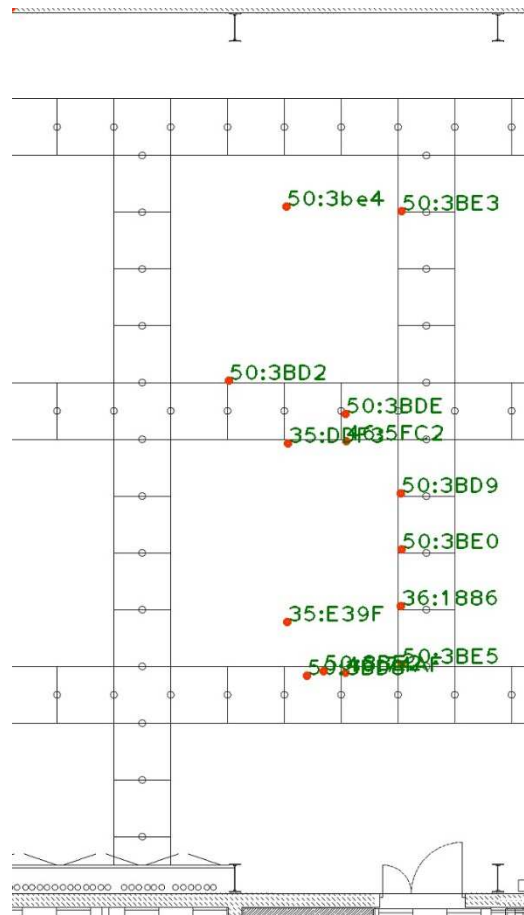


Figure 44: Camera 2: real-world positions of Active RFID Tags computed by distortion compensation and perspective transform algorithm

As presented above, the algorithm has localized each of Active RFID Tags properly. Accuracy can be estimated at about 5 cm. As expected, two correlations were observed:

- Accuracy perspective transformation decreases when the object is further from camera.
- Lens distortion is significant at the corners and margins of frames (despite of distortion correction).

Taking it into account, the best accuracy is observed in the near-middle of each frame. In this demonstration, each tag was captured in both of the cameras, so some of them lie very close to the frame borders.

4.2.1.3 Future work and conclusions

The performed experiments have confirmed that the computer vision subsystem can provide reliable and efficient positioning procedure. Most of the problems can be overcome by tuning the algorithm parameters and setting up cameras properly. However, a few conclusions have been noticed.

- Light source has to be chosen carefully. For example, it was observed, that the best color for LED light source is red and the worst is blue color when using the described cameras. Furthermore, LEDs should provide wide light angle or some diffusors should be used to ensure that light is radiated to the camera with enough strength.
- It is worth considering to use a lampshade to provide high contrast between LED and background.
- Camera's lens calibration is mandatory, because distortion can significantly spoil the result especially in wide angles.

In the future it's planned to increase the experimental area and use more camera devices. It's planned to examine more light sources and camera lenses. Also the calibration procedure will be improved and more algorithms are planned to be tested.

4.2.2 RFID switch measurements

Adding additional signal switching device to UHF RFID reader allows to attach more than two antennas (one for signal receiving and one for transmitting) to one reader. This solution allows to implement a simple method of localization which is based on switching signal between antennas. With signal switching device (Figure 45) one reader may also replace many readers what is important due to space saving and lower cost of implementation. Such reader can be visible by the system as several separate virtual readers. For now, up to eight antennas are possible to be connected to the reader.

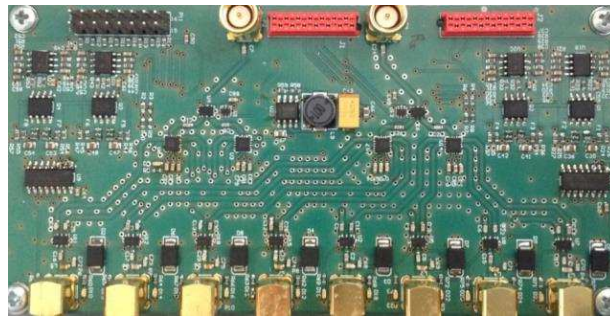


Figure 45: Switching signal module (designed in GUT)

If more than one antenna is in use, it is necessary to determine the time period in which the reader is able to perform passive tag readout. During this time tag has to be excited and its response has to be received by UHF RFID reader. In Figure 46, simplified diagram of passive RFID system [22].

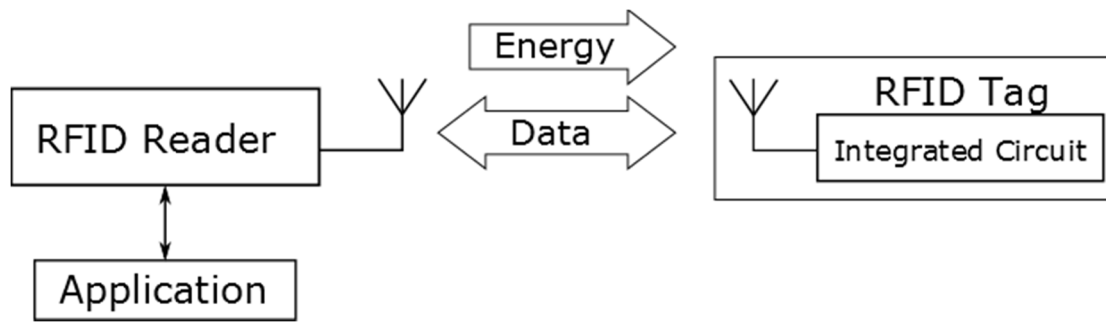


Figure 46: Simplified diagram of passive RFID system

It is important to determine minimum time period in which the passive tag can be read. An experiment was conducted and measured success ratio (calculated as the number of tag readouts divided by the number of antenna switches) is presented in Figure 47. During the experiment RFID Reader was set to continuous work and the antennas were switched by external interface.

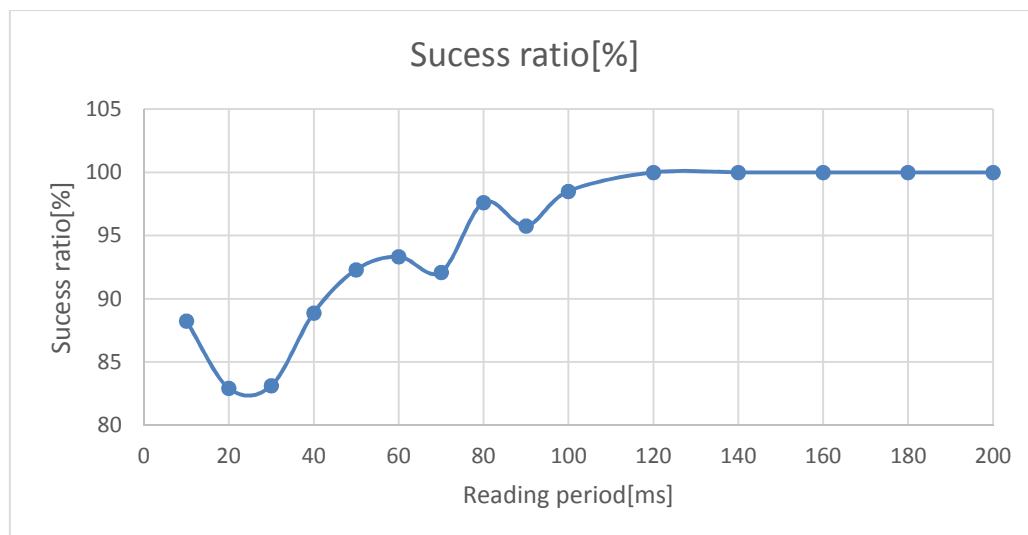


Figure 47: UHF RFID Tag readouts success ratio(see text for explanations)

As a result of the experiment, minimum time period for one antenna was determined as 120 ms. In order to avoid switching of the antenna during readout process and decrease readouts failures, switch control has been implemented in UHF RFID reader's microcontroller. Tests of new implementation are in progress.

4.2.3 RFID ESPAR antenna

ESPAR (Electronically Steerable Parasitic Array of Radiators) is switched beam antenna. ESPAR arrays are suitable for positioning systems where determination of the direction of the incoming signal is required. ESPAR antenna has a simple construction with one active element surrounded by a defined number of passive elements and provides 360° beam control in steps. Radiation characteristic switching

is performed by SPST switches (ON/OFF) that have to provide required load for the parasitic elements. By adequate RF switches configuration obtaining a directional beam is possible [23].

The ESPAR antenna adapted to cooperate with UHF RFID Reader (868 MHz) was designed and fabricated by GUT. In Figure 48 antenna realization is presented.

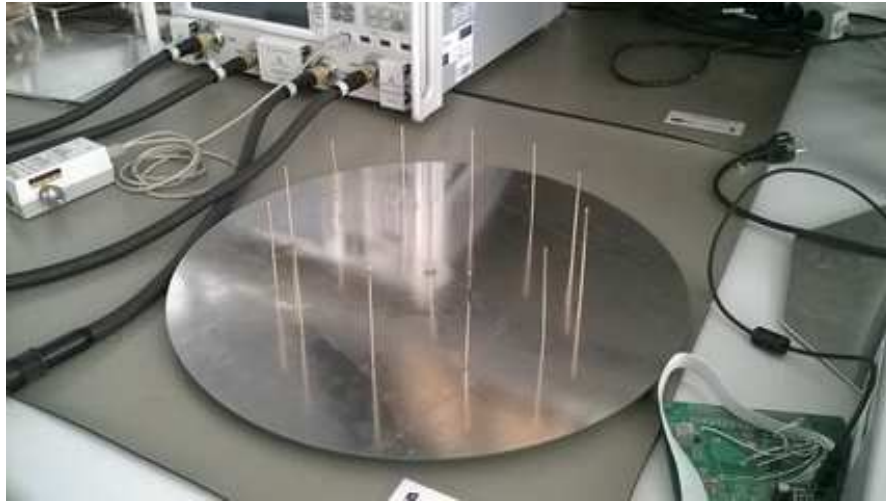


Figure 48: ESPAR antenna (designed in GUT) - top view

The radiation pattern and input impedance matching for three different configurations of ESPAR antenna were measured (Figure 49, Figure 50). The measurements were made in the anechoic chamber for three different configurations and the simulations were made for one configuration due to symmetry of the antenna. Each of configurations consists of five directors and seven reflectors.

In order to validate ESPAR antenna directivity, several measurements were performed. In Figure 45, exemplary areas of passive RFID tag readouts are presented. Each measurement was performed with different height above ESPAR antenna.

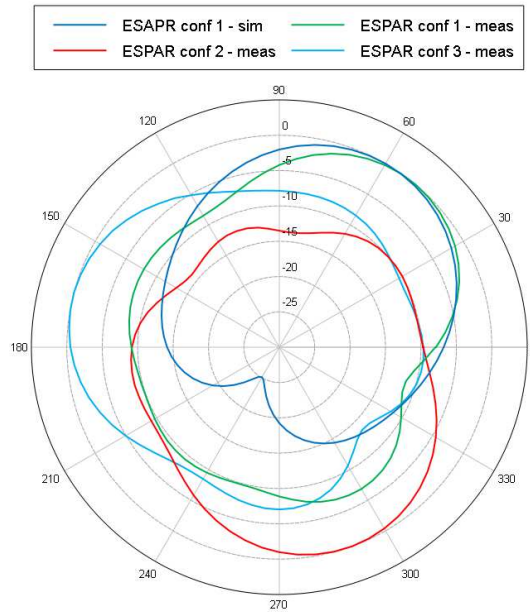


Figure 49: Radiation patterns at horizontal plane for $\theta = 60^\circ$

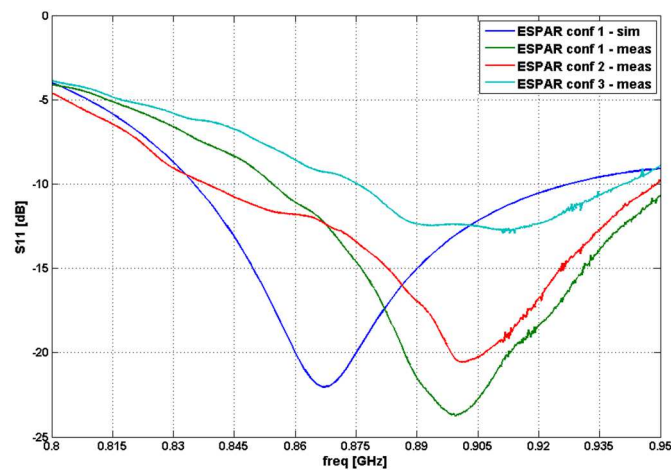


Figure 50: Antenna input impedance matching characteristics

The measurement's results show that designed and manufactured antenna has similar parameters. Antenna is well matched for all free configurations and is able to cooperate with UHF RFID Reader.

In order to validate ESPAR antenna directivity several measurements were performed. In Figure 51 one can see exemplary areas of passive RFID tag readouts. Each measurement was performed with different height above ESPAR antenna.

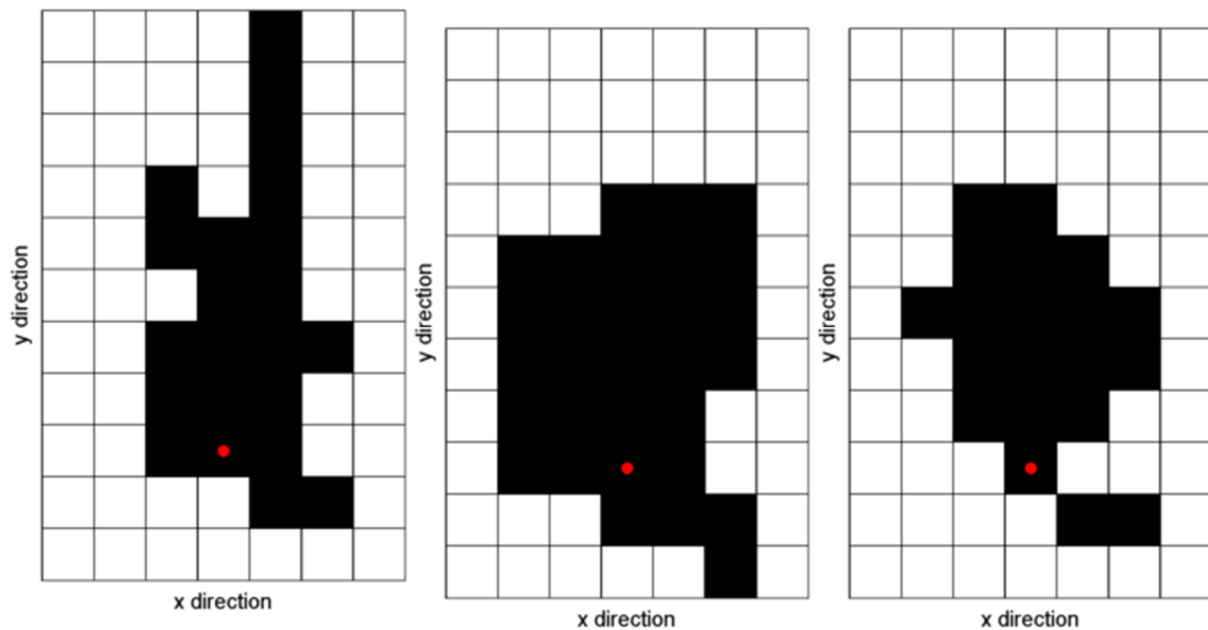


Figure 51: Areas of passive RFID tag readouts measured on different heights above ESPAR antenna (respectively 0.5 m, 1 m and 1.5 m), red dot indicates antenna position

The measurement's results show that estimation of passive UHF RFID tag direction is possible when using designed antenna. In future work performance of localization algorithms will be tested when using UHF RFID reader with dedicated ESPAR antenna.

4.2.4 RF based localization

Three testbeds in three environments were prepared in order to measure how performance of different RF localization algorithms is influenced by change in RF signal propagation conditions.

Physical layer of the first testbed is based on an anechoic chamber which is a part of the laboratory available at the Faculty of Electronics, Telecommunications and Informatics, Gdansk University of Technology. To confront anechoic chamber measurements with the results obtained in commonly used test sites, two more testbeds were prepared. Office test site 1 (later called "office_1") contains a typical office room equipment including furniture and computers. On the floor the same measurement grid as in the anechoic chamber was deployed and also a part of anechoic chamber measurement equipment (columns and wireless modules with batteries) were used. Office test site 2 (later called "office_2") is the third measurement environment, which has the most challenging conditions for a localization system with respect to RF signal propagation. It consists of two rooms with 30 cm width wall between them and high density of furnitures, computers and other equipment not present in the office test site 1.

In figures below (Figure 52, Figure 53, Figure 54, Figure 55) and Table 10 results of localization process (in the form of cumulative distribution function, value 0.8 on y axis indicates that 80% of

measurements have localization error lower than the value indicated by x axis), performed with the use of data gathered from four modules installed respectively in prepared testbeds, are presented. In all testbeds relative placement of reference modules and measurement points were the same. For localization purposes Multilateration [24], MLE [25], WCL [26] and fingerprinting [27] algorithms (described in deliverable D3.6) were implemented and localization processes were performed.

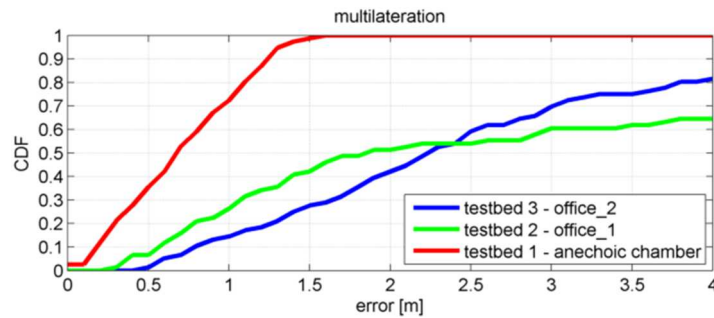


Figure 52: Localization results of multilateration algorithm calculated in three testbeds

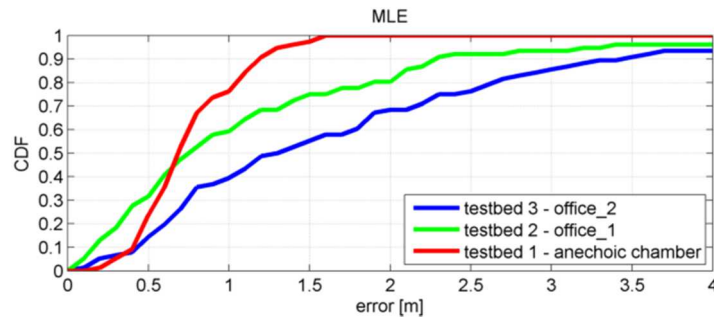


Figure 53: Localization results of MLE algorithm calculated in three testbeds

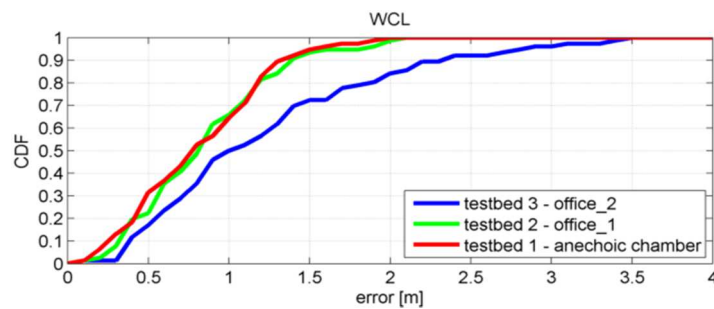


Figure 54: Localization results of WCL algorithm calculated in three testbeds

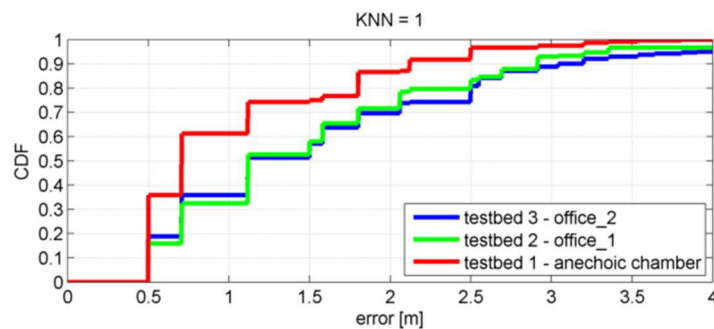


Figure 55: Localization results of KNN = 1 algorithm calculated in three testbeds (fingerprinting map with 1 m spacing).

The presented result shows how external environment influences results of positioning that is based on implemented algorithms and RSS measurements. Change of external conditions has different influence on each of the algorithms. Multilateration was an algorithm that is the most sensitive on hard propagation conditions while WCL and fingerprinting presented less change in accuracy. The obtained results are listed in Table 10.

Table 10: Localization results obtained in three testbeds

algorithm	CDF value	anechoic chamber	Office_1	Office_2
		localization error [m]		
Multilateration	0.5	0.68	1.85	2.23
	0.8	1.10	>4	>4
	0.9	1.25	3.80	>4
MLE	0.5	0.69	1.05	1.20
	0.8	0.75	2.00	2.30
	0.9	1.30	2.65	3.42
WCL	0.5	0.76	1.19	1.35
	0.8	0.78	1.19	1.39
	0.9	1.00	1.90	2.32
KNN=1	0.5	0.73	1.80	2.12
	0.8	1.12	2.49	2.91
	0.9	1.12	2.50	3.06

In future work more tests of RF localization algorithms in different environments will be performed to provide solutions that are best suited for T5.2 demonstrator.

4.3 Augmented reality task (TED)

In addition to the setup of the COPCAMS computing board, the TED use-case involves additional hardware, such as the Oculus Rift virtual reality headset and the OVRvision stereo camera. The communication with both elements has been tested paying special attention to the latency, since it is well known that latency not only degrades the virtual reality experience but also causes eye fatigue and motion sickness.

A test application has been developed using Unity 5 which can show the stereo image from the cameras in Oculus Rift virtual reality headset with scalable and legible text in an overlay (Figure 56). This program is being used to determine the best configuration for easy reading and user interface distribution within the field of vision, a non-trivial task due to Oculus DK1's low display resolution.

The preliminary experiments show that the setup achieves an acceptable user experience. However, further tests will be needed, since at this point the object recognition middle-ware is still under development and such layer will introduce additional delays in the system.



Figure 56: Stereo display with direct video feed and overlaid text

Regarding the image processing algorithms involved in the prototype, just the distortion correction and basic prototypes of a key point based model matching algorithm have been tested on the computing board. None of them has been optimized nor parallelized yet, so at this point no accurate estimation of their processing times is available.

Although the bankruptcy of the Spanish leader has led to important delays, TED expects to provide a parallelized version of the distortion correction and image rectification algorithms in the following weeks that will be reported in D3.4. On the other hand, the object detection algorithms are still in an early stage and further efforts are needed, not only to improve recognition rate, but also to improve performance. In D4.4 the key point based model matching algorithm is presented and some insights about this ongoing work are provided.

4.4 Robot tracking task (UC)

In WP3 some different works related with image processing have been done, these labour is closely related with the use case and system presented above. On the following lines, it is going to be explained briefly how this image processing algorithms are currently used on the different data flow of the system, stage by stage. The results of these experiments are also included in deliverables 3.1, 3.2, 3.4, and 3.5.

Stage 1: Input data from the environment

The algorithm captures image from camera and transforms the pair images into rectified and undistorted images to compensate nonlinear effects of the lens, such as radial and tangential lens distortion (Figure 57). Then, image quality is improved by removing sensor noise (Figure 58), in order to reduce to a minimum the mismatches between the left and right images.



Figure 57: Rectified and undistorted images



Figure 58: Noise removal from an image

Stage 2: Detect movement and markers

Use an image algorithm to detect the proposed reference markers (LED light + black contrasting surface), which are in different light conditions and on different distances from the camera (Figure 59).



Figure 59: Markers detection

Stage 4: Frontal movement (stereo)

By the use of stereo cameras and epipolar geometry, get the 3D coordinates of the object to characterize (Figure 60). It is necessary to apply stereo mapping or stereo matching, look for the same point in both images; and calculate projective or epipolar geometry (Figure 61), by describing the relationship between the image planes (Table 11) of the camera and the point.

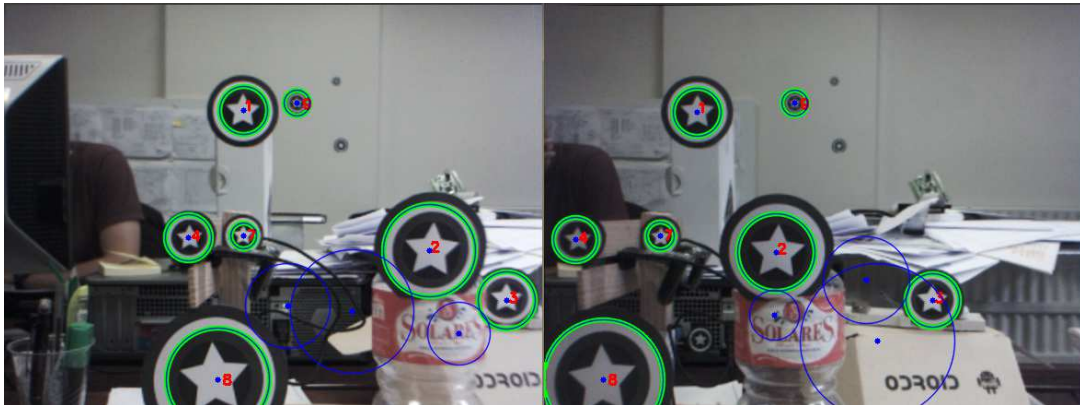


Figure 60: Stereo matching



Figure 61: Example of a bottle depth obtaining

Table 11: Relationship between the image planes

Left image coordinates	u = 546 v = 269	Bottle's depth $z = \frac{focal_length \times baseline}{disparity} = 37,13\ cm$
Right image coordinates	u = 328 v = 269	

5 Validation

5.1 State of the art at project start

This section describes the state of the art in the field of smart cameras and embedded systems at project start. It focuses on advanced manufacturing applications examples with emphasis on the quality control, RFID object positioning applications and Augmented Reality tasks.

5.1.1 Quality control tasks (KTOR, JSI)

In the research and development of industrial vision systems, most applications are related to inspection. There are five types of inspection:

- a) inspection of surface quality,
- b) inspection of dimensional quality,
- c) inspection of correct assembling (structural quality)
- d) inspection of accurate or correct operation (operational quality).

Surface quality inspection includes inspecting the objects for scratches, cracks, wear, and checking surfaces for proper finish, roughness and texture. This type of inspection is used in textile, wood and metal industries by employing vision systems for fault detection and quality verification [7][8][9]. Inspection of dimensional quality includes checking whether the dimensions of an object are within specified tolerances or the objects have the correct shape. More precisely, the vision systems check geometrical characteristics of objects, such as dimensions, shape, positioning, orientation, alignment, roundness and corners in two or three dimensions. Examples of inspection of geometrical characteristics are reported in [10][11][12]. Structural quality inspection includes checking for missing components, e.g., screws, rivets, etc., on assembled parts or checking for the presence of foreign or extra objects, e.g., leaves, little sticks, dust, etc. Examples of structural quality inspection are presented in [13][14][15]. Inspection of operational quality consists of verification of correct or accurate operation of the inspected products according to the manufacturing standards. Examples are described in [16][17].

There exist also all-in-one embedded machine vision solutions that integrate image capture and image processing together with built-in software to provide quality control and improved productivity for manufacturing operations [18]. Such solutions can be applied across a wide range of industries such as agriculture [10], automotive [19], and electronics [20].

On the market, we can find several manufacturers that offer smart camera solutions for industrial usage. The companies Keyence, Cognex, National Instruments and Sick dominate the market of

commercially available smart cameras in terms of hardware solutions with implemented dedicated software. However, the majority of these solutions use its own hardware, which is based on the embedded x86 PC, with integrated commercial available CPUs (e.g. INTEL Atom x86). Consequently, these smart cameras are not offering the state-of-the-art performance regarding the computational performances and power consumption.

The company XIMEA was the only company found at the start of the COPCAMS project (April 2013), which was offering a commercial industrial smart camera embedded vision system, with both CPU and GPU cores on a single die. The company claims that their smart camera CURRERA-G by using GPU cores can deliver 90 GFLOPS of processing power. Furthermore, they offer application programming interfaces (APIs) for 30 of the most common image-processing libraries including OpenCV.

At the start of the COPCAMS project, all implemented machine vision solutions in KTOR production facilities were PC-based. KTOR is using its own computer vision software called Kolektor Imaging Software (KIS), which is essentially a framework that combines specialized machine vision algorithms (operators) frequently used in commutator production. In addition, in KTOR production for non-complex machine vision inspections, smart cameras from companies like COGNEX are used.

The next generation of smart camera systems including the embedded platforms from the COPCAMS project will enable the deployment of significantly improved computer vision algorithms enabling more accurate real-time inspection of products. Moreover, the network of cameras will enable improved inspection of products by taking into account the sequential nature of a manufacturing processes, and make it possible to analyze the (inter)dependencies of various steps of the process and the impact of the steps on the quality of the final product. Implementation of the proposed quality control system will result in higher quality of products and increased productivity. In addition, it will be possible to adapt the developed system for deployment on other production lines during or after the project.

5.1.2 Object positioning task (GUT)

During the research, it was observed that most of the applications and systems, which are considered as “intelligent surveillance systems” deliver common set of functionalities. The main goal of intelligent video surveillance is to extract useful information from video stream collected by cameras deployed in factories, at airports or any other place where video surveillance is being used. Intelligent surveillance systems deliver possibility of [28][29]:

1. Multi-camera calibration

Mapping different camera views to a single coordinate system.

2. Object re-identification

Matching two image regions observed in different camera views and recognize whether they belong to the same object or not.

3. Multi-camera tracking

Tracking object across the field of view of different camera.

4. Multi-camera activity analysis

Recognition of activities of different categories and detection of abnormal activities in a large area by fusing information from multiple camera views.

Intelligent surveillance systems are used in multiple places, where real-time alerts and the ability to search specific items, are based on their unique characteristic. Thus intelligent surveillance systems are popular in public places, such as train stations, airports, crowded streets and, on the other hand, such systems are used in industry. When considering market-ready device-embedded systems, it is worth to mention:

IOImage released the IOIcam xptz100dn, an IP pan, tilt and zoom (PTZ) camera with autonomous tracking capabilities. Intelligent IOIcam is day/night, all-weather camera with embedded built-in analytics that delivers cost-effective intelligent solution. IOIcam is able to automatically detect, track objects such as vehicles, people etc. [30].

Agent Video Intelligence (Agent Vi) has completed the integration with Axis Communications' camera application platform and it's available as an embedded solution. Agent Vi performs real-time analysis of the video stream captured by camera. On that basis it identifies and generates alerts for user predefined events related to people, vehicles and objects. Video-search capabilities enable rapid and effective retrieval, analysis and presentation of specific Video segments, events and data from vast amounts of recorded video [31].

Bosch IVA 4.0 is the security assistant system for indoor and outdoor use. IVA 4.0 detects, tracks and analyzes moving objects while suppressing unwanted alarms from spurious sources in the image. IVA 4.0 is an embedded system prepared in Dinion IP, Extreme IP, FlexiDome IP, and AutoDome IP cameras [32]. The system

- detects idle/removed object, loitering, and linecrossing,
- displays/detects object trajectories, speed, direction, heads and color,
- optical flow detection of objects in a surveillance scened

- creates metadata for forensic searching of recorded video.

It is observed that for industrial purposes intelligent surveillance video systems are integrated with RFID systems (1, 2, 3, 4). One of the first deployment of tracking system for industrial needs, based on RFID linked with CCTV, took place in 2006. Sony Europe (1) installed a monitoring system that helped reduce theft of warehouse goods, but also increased the efficiency of Sony's shipping processes. The company installed the system at its largest European distribution warehouse in Tilburg, the Netherlands [33].

Nox solution (2), delivered by SimplyRFID, integrates video surveillance system with passive RFID tags. Nox searches video by location, camera, time, and RFID-triggered events. Video can be located when an RFID tagged item was seen in the video, when the item missing, when an item was checked in/out, or when an item caused an alarm. Nox plays video and shows all RFID tagged items in-view at time of the video being recorded, by each individual frame of the video. Video can be played forwards, backwards and in-real-time [34].

GuardRFID delivers software applications, such as TotGuard™ Infant Security (3), integrated with Active RFID platform. Security and access control systems are enhanced by presenting a live video stream from a CCTV camera placed at the location associated with an alarm or warning event within a system, as well as providing video images of activity in that location immediately prior to the event. The alert (event) generated by the RFID tag is supported with a real-time video image and archived records to become an integral part of patient monitoring. Instantaneous visibility of such activity allows staff to immediately respond to the event, saving precious time. All such video streams are captured and archived for subsequent review, if ever required [35].

Within the scope of the project the two companies Dallmeier and initPRO (4) work on the integration of RFID data into video images for tracking flow of goods in warehouse. Data which are transmitted by the RFID tag such as date, time or serial number can be integrated into the video image. For this purpose the RFID reader sends data to the Dallmeier recorder via Ethernet. The data is then displayed within the management software PView, either in or next to the video image [36].

Intelligent surveillance video integrated with RFID technology is not commonly used solution in industry. On the other hand, the Sony case shows that it can reduce financial losses as well as improve operational efficiency. RFID technology in the presented examples is used to track objects and assets, based on passive tags. COPCAMS uses active RFID to provide close to real-time information about assets' localization. Integration of optical methods of object tracking with active and passive RFID tracking allows computer vision algorithms to identify and locate tracked assets and gives an opportunity to increase the reliability and accuracy of the whole positioning system, especially in industrial environments where localized objects cannot be present in the line of sight. What also makes a difference

is that in the presented examples (1, 2, 3, 4) processed localization, visual and radio data are collected in the computational server. COPCAMS allows to deliver the same value, based on a distributed system of Smart Cameras with RF sensing capabilities, where information is processed on the device. Such an approach allows to scale the surveillance system by simply adding new Smart Cameras with RF sensing capabilities without investing in increase of existing computing power infrastructure. Additionally, as Smart Cameras with RF sensing capabilities can cooperate, with increasing number of devices the overall positioning performance can increase (depending on devices placement and environmental conditions). Integration of camera with efficient mSoC allows for removal of band consuming, time and energy inefficient process of encoding, transfer and decoding video data, which is necessary when high quality video data has to be processed on an external server. Combination of possibilities of video and various radio frequency techniques allows for adjustment of Smart Camera with RF sensing capabilities system to end-user needs.

5.1.3 Augmented reality task (TED)

There are few experiments exploring the use of augmented reality on industrial applications, but to the best of our knowledge no commercial developments are available. As the main limitation, all depend on heavy computing equipment, making them unpractical for field deployment. An example proposal can be found at <http://monet.cs.columbia.edu/projects/armar/>.

5.1.4 Robot tracking task (UC)

In the recent years, there has been a growing interest in the systems and products related to the location of objects in three dimensions (3D). The sectors covering this technology are very broad, such as robotics, medicine and games, among others.

To know the precise position of an individual, the systems may be based on the use of cameras, optical sensors, accelerometers, gyroscopes, GPS, etc. In the event that vision systems are used, it is necessary to perform a pre-processing of the region of interest where the individual is located using imaging algorithms that detect corners, edges or reference markers; then, with these data is possible to obtain the real 3D coordinates of the environment.

One of the problems that have been found in other studies [38] when using markers, is light in the environment where the images will be taken. The points to be detected in the scene may be lost because of the darkness. This limits the applications that use this system indoors. Furthermore, the use of contrast enhancement algorithms and specific markers stored in a database is required, which substantially increases the computing time of these systems. In addition, it limits significantly the distance between printed markers and the system user, unless its size is large enough to be captured by the image sensor. To solve this problem, light markers working in the visible or infrared spectrum can be used, such as

light emitting diodes or lasers. In some cases [39], light sources with varying luminance or pulsed light have been proposed which can cause synchronization failures. Still, the use of luminous markers can pose problems, particularly in environments where light sources with much higher luminance than the marker itself (in the worst case, sunlight) or sources emitting radiation in the same direction are present. In such situations, the image sensor is not able to differentiate one light source from another, so it will force, as was previously the case, to use this technology in bright environments without big light sources in it. Therefore it will be necessary to introduce element positioning systems that prevent light conditions affecting an environment so significantly.

In the article [37] it is proposed to incorporate infrared luminous markers on a tape on the head user. To do this, they put on the scene two independent cameras, which require a synchronization process to make the shot simultaneously, located at a distance equal to the length of the wall of the room where tested. The algorithm used to make an estimate of the position is based on stereo correspondence. One of the drawbacks is that it cannot be implemented for augmented reality systems or simulated, because the cameras do not show what the user sees, besides being restricted to indoor environments with limited dimensions.

Other studies as "Tracking of user position and orientation by stereo measurement of infrared markers and orientation sensing" (M. Maeda, et al., Proceedings of the 8th International Symposium on Wearable Computers (ISWC'04), 2004) raises the use of infrared markers located on the wall of a room, to locate the user. Specifically, they propose the use of two types of markers: actives and passives. The active markers are formed by a set of three infrared LEDs and a signal transmitter that sends data from its actual position to a decoder that the user carries, so once the detected know their absolute position. The passive markers are only one source of infrared light, from which it obtains the relative user position. In addition to relying on receiving signals from active markers, it calculates the relative distance from stereo vision. Using this technique, as occurred in the cases discussed above, it is restricted to indoor use.

There are other methods that do not require direct vision of one or more cameras with reference markers for locating and tracking individuals. The RF techniques involve measuring distances, from static or moving objects, by emitting electromagnetic pulses that are reflected on a receptor. These electromagnetic waves are reflected when significant changes in atomic density between the environment and the object, so that works particularly well in cases of conductive materials (metals). They are able to detect objects at greater distances than other systems based on light or sound; however they are quite sensitive to interference or noise. It is also difficult to measure objects located at different distances from each other to the transmitter, because the pulse frequency will vary (slower the farther and vice versa). However, there are experimental studies which are able to demonstrate its use to estimate the user location with a high level of accuracy.

Another example of existing solutions are the LIDAR systems, which calculate the distance through the time taken for a light pulse to be reflected on an object or surface; using a device with a pulsed laser such as a light emitter and a photodetector as a receptor of the reflected light. The advantage of these systems is the accuracy achieved over large distances (using lasers with wavelength > 1000 nm) and the possibility of mapping large area lands by scanning light pulses. The disadvantages are that it is necessary to analyze and process each point, and the difficulty of automatically reconstruct three-dimensional images.

5.2 Targets at project end

5.2.1 Quality control tasks (KTOR, JSI)

The selected field tests will be implemented in KTOR facilities. Field tests will be installed at the production line at different production phases of the graphite commutator. Dedicated software and hardware (automatization, manipulation) for each field test will be developed. The overall objective of quality control tasks is to develop applications for quality control of the specific production processes, which will be able to detect defects on the commutators during the production. In order to validate the solutions developed during the COPCAMS project, the field tests will be running for a longer period (e.g. 3 months).

5.2.1.1 Objectives and goals

Objectives and goals for a quality control tasks can be divided to COPCAMS project objectives and applications/field tests specific objectives.

COPCAMS project:

- Cost reduction of the machine vision systems in comparison to the current PC-based systems used in KTOR (less expensive hardware, no additional licensing needed, and consequently enabling implementation of the quality control in every phase of the production process)
- Reduced power consumption for automated visual inspections by 50% (replacement of currently used PC-based machine vision systems with the COPCAMS solutions)
- Shortening the development cycles of complex machine vision projects by 15 % (due to the reusable hardware and the methodology developed during the project)
- Self-adaptivity (learning on newly collected data)

Application specific objectives:

- Achieving of acceptable classification accuracies according to the prescribed tolerances (confusion matrix of the deployed classification model)
- Reduction of product rejection rate, resulting in savings in material and energy
- Higher quality of manufactured products

5.2.1.2 Evaluation and evaluation strategy

Each objective will be measured and evaluated during the implementation of the field tests. From the application point of view, the main success criterion for acceptance of the developed algorithm/application will be quality-control accuracy.

5.2.2 Object positioning task

The system will be installed and tested in KTOR facility placed in Idrija, Slovenia. Smart Cameras with RF sensing capabilities and other sensors will be deployed. It is planned to conduct a series of testing sessions. During the tests, functionalities of system of Smart Cameras with RF sensing capabilities will be validated, while the system will provide close to real-time information about assets positions.

5.2.2.1 Objectives and goals

Objectives and goals for a quality control tasks can be divided to COPCAMS project objectives and applications/field tests specific objectives.

COPCAMS project objectives:

Use of embedded computing platform (TI KeyStone 2) in the system that is being developed allows to eliminate the bandwidth, energy and time cost associated to process of encoding, transmission and decoding of video data that is necessary if video data from IP cameras is processed on central server like in systems that were available at the start of the project.

Application specific objectives:

During the field tests, the system will provide close to real-time localization of predefined assets. This information will be provided to KTOR facility employees.

5.2.2.2 Evaluation and evaluation strategy

COPCAMS project objectives:

The amount of data that is sent from camera to the server that is storing calculated positions will be measured in two scenarios. For each of the scenarios the same combinations of video parameters, such as resolution and FPS, are planned to be tested. In the first scenario, after triggering positioning process, the IP camera will send the video data to the server where Computer Vision algorithms will be implemented and the position of active RFID tag will be calculated. The process will be repeated for each configuration and after each of procedures the amount of transferred data will be determined. In the second scenario, after triggering the positioning process, the smart camera will process video data and send information about the calculated position of active RFID tag to the server. As before, the amount of transferred data will be determined for each configuration. After the measurements the amount of transferred data for each configuration in both scenarios will be compared.

Application specific objectives:

The measure of success will be the amount of successfully localized objects with satisfying accuracy and delay of the whole localization process. The accuracy of the system will be dependent on quality of calibration, number and placement of Smart Camera with RF sensing capabilities devices that will be deployed in T5.2 demonstrator. The target average localization error is expected to be less than 3 m for measurements in the most challenging case when the tag that is expected to be localized is not in the line of sight of any of the cameras and only RF information is available. Moreover, KTOR facility employees will provide the overall impression of system's performance.

The main strategy of system evaluation will be location measurements of objects in predefined locations. Due to the fact that measurement of many objects at the same time and comparing with simultaneously gathered real positions measurement is difficult, the proposed strategy will be applied. Objects will be placed in predefined locations and the measurement process will be triggered. After the finish of each localization process, the estimated location will be compared with real location and the localization error will be calculated. Also for every localization process, the delay between localization trigger and delivery of result will be measured.

5.2.3 Augmented reality task (TED)

The objectives of the virtual reality demonstrator can be divided in two categories. On the one hand we have the objectives from the technological point of view:

- Take full advantage of HW
COPCAMS provides a low power, reduced cost, high performance image processing platform that leverages the capabilities of the virtual reality application being developed by TED. The implementation of multi CPU and GPU optimized algorithms will allow to take full advantage of the hardware capabilities.
- Portability
Although external causes have forced TED to leave the STORM platform and move to a non-portable platform, portability is still a key factor for TED. The use of COPCAMS technologies ensures an easy path towards future portable solutions.

On the other hand we have the objectives from the usability point of view:

- Latency of the video-feed
Low latency of the video-feed is needed to achieve a virtual reality experience. Moderate latency causes eye fatigue and motion sickness. High latency dramatically degrades the virtual reality experience making the system unusable. TED expects to achieve the required low latency thanks to the COPCAMS technologies.
- Latency of the object recognition middle-ware
Object recognition requires intensive processing and might affect the video-feed latency in several ways. It seems reasonable to use less frames per second for object recognition than for the video-feed. The final application must take this into account, decouple both elements, and find an equilibrated balance that optimizes usability.
- Overlay quality
The user interface should be intuitive, provide clear information and be easy to interact with.
- Object recognition success
The recognition of objects has to be reliable and provide a low rate of false positives and false negatives.

Further details about objectives and field tests related to the augmented reality demonstrator can be found in D1.4.

6 Current state of the demonstrator

6.1.1 Quality control tasks (KTOR, JSI)

Dimensional measurements task

A dedicated machine vision algorithm has been ported to the Nvidia Jetson platform and tested on the offline captured images. To enable an operator on the production line to observe results of the current inspection, a GUI application was built. The initial results (detection rate) obtained in the laboratory are satisfactory, however the final evaluation of the success criteria will be possible after the implementation of the system on the KTOR production line. Implementation of the system will start in M31 and will be finished before the end of M36.

Quality inspection of copper-graphite soldering

Basic machine vision algorithms for detection of the defects in the soldering process were ported to the Nvidia Jetson platform. Tests on the larger acquired dataset of images were performed. Some product defects are detected very successfully, while some (deficit of solder) will need additional tuning. In addition, a lot of effort is currently invested in building of the mechanical manipulator, which will enable implementation of the system on the production line. Implementation of the system will start in M32 and will be finished before the end of M36.

Measurement of the commutator mounting holes roughness

Machine vision, machine learning and optimization algorithms were ported to the Nvidia Jetson platform (OpenCV and CUDA). The first version of the application for roughness measurement was built and tested on the offline captured dataset of images. In order to improve the assessment of the mounting hole roughness, some additional tests will be performed (optimization of the machine learning algorithm parameters). Implementation of the system on the production line will be performed within the following months.

6.1.2 Object positioning task (GUT)

Early prototypes of all system components described in Section 3.2 (Object positioning task) are developed or are very close to their final version. More detailed information about the actual state of the algorithms and hardware are available in deliverables D3.6 and D4.4. The first demonstration of an early system prototype that will show the basic system functionality is planned for the second COPCAMS review in Gdansk.

6.1.3 Augmented reality task (TED)

The cameras and the virtual reality headset used in the prototype have been integrated and tested.

A parallelized version of the distortion correction and image rectification algorithms is ongoing. It is expected to be finalized in the following weeks and reported in D3.4.

The object detection algorithms still require further refinement. The optimization of the algorithms to the COPCAMS platform will begin once their development is finalized.

7 Conclusion

In this deliverable, we summarized the demonstration tasks and provided specifications in advanced manufacturing applications in the COPCAMS project. We provided a detailed description of the demonstration tasks that will be implemented during the project. Demonstration tasks form four different areas as specified (field tests and prototype demonstrations): quality control tasks, RFID tracking task, augmented reality task and robot tracking task.

Each use case (field test or prototype) will validate and demonstrate the technologies developed during the project. The methodology, architecture and initial results of experiments are presented in this deliverable, however the detailed analysis of the evaluation results will be presented in deliverable *D5.5 Advanced Manufacturing Applications Report* at the end of the project and will be based on the success criteria defined in the document D1.4.

References

- [1] E. Dovgan, K. Gantar, V. Koblar and B. Filipič. Detection of Irregularities on Automotive Semiproducts, Proceedings of the 17th International Multiconference Information Society, IS 2014, vol. A, pp. 22–25, October 2014.
- [2] V. Koblar and B. Filipič. Designing a quality-control procedure for commutator manufacturing, Proceedings of the 16th International Multiconference Information Society, IS 2013, vol. A, pp. 55–58, October 2013.
- [3] V. Koblar, E. Dovgan and B. Filipič. Tuning of a Machine-Vision-Based Quality-Control Procedure for Semiproducts in Automotive Industry, Submitted for publication, 2014.
- [4] T. Robič and B. Filipič. DEMO: Differential evolution for multiobjective optimization, Proceedings of the Third International Conference on Evolutionary Multi-Criterion Optimization, EMO 2005, pp. 520–533, March 2005.
- [5] R. Storn and K. V. Price. Differential evolution – A simple and efficient heuristic for global optimization over continuous spaces, *Journal of Global Optimization*, vol. 11, no. 4, pp. 341–359, 1997.
- [6] I. H. Witten, E. Frank. *Data Mining: Practical Machine Learning Tools and Techniques*. Second Edition. Morgan Kaufmann, San Francisco, 2005.
- [7] M.S. Packianathe, P.R. Park, Neural networks for classifying images of wood veneer, Part II, *International Journal of Advanced Manufacturing Technology* 16 (2000) 424–433.
- [8] K.L. Boyer, T. Ozguner, Robust online detection of pipeline corrosion from range data, *Machine Vision and Applications* 12 (2001) 291–304.
- [9] D.M. Tsai, C.Y. Hsieh, Automated surface inspection for directional textures, *Image and Vision Computing* 18 (1999) 49–62.
- [10] A.R. Jimenez, R. Ceres, J.L. Pons, A vision system based on a laser range-finder applied to robotic fruit harvesting, *Machine Vision and Applications* 11 (2000) 321–329.
- [11] S. Anard, C. McCord, R. Sharma, An integrated machine vision based system for solving the nonconvex cutting stock problem using genetic algorithms, *Journal of Manufacturing Systems* 18 (1999) 396–414.
- [12] H.K. Tonshoff, C. Soehner, G. Isensee, Vision-guided tripod material transport system for the packaging industry, *Robotics and Computer- Integrated Manufacturing* 13 (1997) 1–7.

- [13] I. Khandogin, A. Kummert, D. Maiwald, DSP algorithms for the automatic inspection of fixing devices of railroad lines, International Conference on Signal Processing Applications and Technology (ICSPAT'98) (1998).
- [14] J. Velten, A. Kummert, D. Maiwald, Real time railroad tie inspection implemented on DSP and FPGA boards, International Conference on Signal Processing Applications and Technology (ICSPAT'99) (1999).
- [15] K.H. Kim, Y.W. Kim, S.W. Suh, Automatic visual inspection system to detect wrongly attached components, International Conference on Signal Processing Applications and Technology (ICSPAT'98) (1998).
- [16] J.Y. Jeng, T.F. Mau, S.M. Leu, Gap inspection and alignment using a vision technique for laser butt joint welding, International Journal of Advanced Manufacturing Technology 16 (2000) 212–216.
- [17] M. Moreira, E. Fiesler, G. Pante, Image classification for the quality control of watches, Journal of Intelligent and Fuzzy Systems 7 (1999) 151–158.
- [18] S. Geraghty, Can Machine Vision be Your Answer? Quality (2010), available online: http://www.qualitymag.com/Articles/Web_Exclusive/BNP_GUID_9-5-2006_A_10000000000000814896
- [19] P. Kellett, Machine Vision in the Automotive Industry, AIA Vision Online (2006), available online: http://www.visiononline.org/vision-resources-details.cfm/vision-resources/Machine-Vision-in-the-Automotive-Industry/content_id/1175/id/2/category_id/60/newsType_id/0
- [20] Automated Optical Inspection and Advanced Vision Solutions: V2000, ViTrox, available online: <http://www.vitrox.com/v2000.aspx>
- [21] Woznica, P.; Tarkowski, M.; Plotka, M.; Kulas, L., "RF indoor positioning system supported by wireless computer vision sensors," in *Microwaves, Radar, and Wireless Communication (MIKON), 2014 20th International Conference on* , vol., no., pp.1-3, 16-18 June 2014.
- [22] Daniel Dobkin. The RF in RFID Passive UHF RFID in Practice. Newnes, 2008.
- [23] Rzymowski, M.; Nyka, K.; Kulas, L., "Enhanced switched parasitic antenna with switched active monopoles for indoor positioning systems," in *Microwaves, Radar, and Wireless Communication (MIKON), 2014 20th International Conference on* , vol., no., pp.1-4, 16-18 June 2014.
- [24] Jahyoung Koo; Hojung Cha;, "Localizing WiFi Access Points Using Signal Strength," Communications Letters, IEEE , vol.15, no.2, pp.187-189, February 2011.

- [25] Patwari, N.; Hero, A.O., III; Perkins, M.; Correal, N.S.; O'Dea, R.J.; , "Relative location estimation in wireless sensor networks," *Signal Processing, IEEE Transactions on* , vol.51, no.8, pp. 2137- 2148, Aug. 2003.
- [26] Pivato, P.; Palopoli, L.; Petri, D.; "Accuracy of RSS-Based Centroid Localization Algorithms in an Indoor Environment," *Instrumentation and Measurement, IEEE Transactions on* , vol.60, no.10, pp.3451-3460, Oct. 2011.
- [27] Kamol Kaemarungsi.: *Design of Indoor Positioning Systems Based on Location Fingerprinting Technique*, PhD, 2005.
- [28] Xiaogang Wang; *Intelligent multi-camera video surveillance: A review*; *Pattern Recognition Letters* 34 (2013) 3-19.
- [29] M. Litzenberger, C. Posch, D. Bauer, A.N. Belbachir, P. Schön, B. Kohn, H. Garn; *Embedded vision system for real-time object tracking using an asynchronous transient vision sensor*; *Digital Signal Processing Workshop, 12th - Signal Processing Education Workshop, 4th*.
- [30] *Ioimage Intelligent Video Analytics - Advanced Edge Based Solution (2011)*, available online: http://www.dvtel.com/UserFiles/File/ioimage/ioimage_brochure_A_mar2011.pdf
- [31] *Video Analytics Applications for the Retail Market - How Agent Vi Can Maximize Store Productivity and Add Value to Your Operations*), available online: http://www.agentvi.com/images/Agent_Vi_-_Retail_Applications.pdf
- [32] *IVA 4.0 Intelligent Video Analysis (2013)*, available online: [:http://resource.boschsecurity.com/documents/Data_sheet_enUS_1557565195.pdf](http://resource.boschsecurity.com/documents/Data_sheet_enUS_1557565195.pdf)
- [33] Bart W. Wiegmans, Johan Visser, Rob Konings, Ben-Jaap A. Pielage; *Review of underground logistic systems in the Netherlands: an ex-post evaluation of barriers, enablers and spin-offs*; *European Transport \ Trasporti Europei* n. 45 (2010): 34-49
- [34] *NOX Product Catalogue (2011)* , available online: http://www.ttsys.com/pdf/NOX-Product-Catalogue_TTS.pdf
- [35] *TotGuard Infant Security System (2011)*, available online: http://guardrfid.com/downloads/TotGuard_Infant_Security_System.pdf
- [36] *Dallmeier RFID Integration*, available online: <http://www.dallmeier.com/en/solutions/partner-solutions/rfid-integration.html> [Date: 02.09.2015].
- [37] Mossel A. et al.; *Wide area indoor optical tracking in unconstrained environments*, 23rd *International Conference on Artificial Reality and Telexistence (ICAT)*, 2013.
- [38] Naimark, L.; Foxlin, E. *Fiducial detection system*. U.S. Patent No 7,231,063, 2007.

- [39] Villar Bonet, Eugenio, et al.; Method and apparatus for 3D spatial localization and tracking of objects using active optical illumination and sensing. (2014).